Government of **Western Australia**
Department of **Mines and Petroleum**

RECORD 2014/4

STRUCTURAL EVOLUTION OF THE YALGOO DOME, YILGARN CRATON, WESTERN AUSTRALIA

by
JN Caudery



Geological Survey of Western Australia

MONASH University

Government of **Western Australia**
Department of **Mines and Petroleum**

RECORD 2014/4

STRUCTURAL EVOLUTION OF THE YALGOO DOME, YILGARN CRATON, WESTERN AUSTRALIA

by
JN Caudery

MONASH University

Perth 2014

Geological Survey of Western Australia

MINISTER FOR MINES AND PETROLEUM
Hon. Bill Marmion MLA

DIRECTOR GENERAL, DEPARTMENT OF MINES AND PETROLEUM
Richard Sellers

EXECUTIVE DIRECTOR, GEOLOGICAL SURVEY OF WESTERN AUSTRALIA
Rick Rogerson

REFERENCE
The recommended reference for this publication is:
Caudery, JN 2014, Structural evolution of the Yalgoo Dome, Yilgarn Craton, Western Australia: Geological Survey of Western Australia, Record 2014/4, 87p.

National Library of Australia Card Number and ISBN PDF 978-1-74168-544-2

Grid references in this publication refer to the Geocentric Datum of Australia 1994 (GDA94). Locations mentioned in the text are referenced using Map Grid Australia (MGA) coordinates, Zone 50. All locations are quoted to at least the nearest 100 m.

About this publication
This Record is an honours thesis researched, written and compiled through a collaborative project between the Geological Survey of Western Australia (GSWA) and Monash University, Victoria. Although GSWA has provided field and sample support for this project, the scientific content of the Record, and the drafting of figures, has been the responsibility of the author. No editing has been undertaken by GSWA.

Published 2014 by Geological Survey of Western Australia
This product is published in digital format (PDF) and is available online at <www.dmp.wa.gov.au/GSWApublications>.

Further details of geological publications and maps produced by the Geological Survey of Western Australia are available from:
Information Centre
Department of Mines and Petroleum
100 Plain Street
EAST PERTH WESTERN AUSTRALIA 6004
Telephone: +61 8 9222 3459 Facsimile: +61 8 9222 3444
www.dmp.wa.gov.au/GSWApublications

STRUCTURAL EVOLUTION OF THE YALGOO DOME, YILGARN CRATON, WESTERN AUSTRALIA.

HONOURS THESIS

JAMES N. CAUDERY

OCTOBER 2013

STRUCTURAL EVOLUTION OF THE YALGOO DOME, YILGARN CRATON, WESTERN AUSTRALIA.

This thesis is submitted as a partial fulfilment of the

Honours Degree of Bachelor of Science,

Department of Earth Sciences, Monash University, Clayton, Australia.

JAMES N. CAUDERY

October 2013

DECLARATION

This thesis contains no material which has been accepted for the award of any other degree or diploma in any university and that, to the best of the candidates knowledge and belief, the thesis contains no material previously published or written by another person, except when due reference is made in the text.

James N. Caudery

October 2013

ACKNOWLEDGEMENTS

This thesis was made possible through the generous contributions and advice from a number of people. My thanks is given to:

Dr. Roberto Weinberg for his assistance and boundless advice as supervisor.

Dr. Ivan Zibra for his advice and support both in the field and out.

Simon and Scott for their tireless efforts as field assistants, and also to Tim, Chris and Pete for keeping me sane in the field and the many nights around the fire.

The team at the Geological Survey of Western Australia led by Stephen Wyche for helping organise logistics, aiding me with work within the office and laboratories, and also to MTD Wingate and CL Kirkland for mounting my zircons and performing the SHRIMP analysis.

Dr. Rachelle Pierson and Dr. Massimo Raveggi for their advice and assistance in the laboratory at Monash.

TABLE OF CONTENTS

ABSTRACT

The Yalgoo Dome is an Archean granitoid dome in a granite-greenstone terrane of the Yilgarn Craton, Western Australia. The formation of such domes has been debated, with difficulties arising as these domes have features which can be interpreted to have occurred through a number of different mechanisms (Yin 2004). This work looks closely at superposed folds versus diapiric emplacement. Using structural geology, in the form of mapping structures in three areas of the dome in detail, this work has derived the history of the Yalgoo Dome. It was initially formed by a tonliate intrusion into the Archean greenstone belt at 2960±10 Ma. This intrusion was made up of a larger body, with smaller offshoots intruding up through the greenstones. The region underwent melting and migmatisation, forming in situ and intrusive leucosomes and felsic melt bands. An early foliation, named S_1, is parallel to the magmatic banding and has been folded isoclinally. This event also produced elongated sheath folds oriented dominantly E-W. It is this deformation that defines F_2. This was followed by an open folding event, F_3. This event included narrow shear zones, which drag and rotate the F_2 folds. At 2752 ± 13 Ma, various granitic intrusions intruded into the same place (Zegers *et al.* 1999). These granitoids incorporated xenoliths from the central tonalite and entrained them into the melt. The melt gradually tore the xenolith apart, resulting in smaller xenoliths all sub-parallel to one another. The contact between the dome and the greenstones is a major shear zone recording normal movement, however complexities arise with a few samples demonstrating reverse movement. This could be associated by porphyroblast re-rotation by a late crenulation cleavage. This research supports the suggestions by Foley (1997), and from that Rey *et al.* (1999),

that the Yalgoo Dome was formed through gradual emplacement of plutons, and rejects the superposed folds model of Myers and Watkins (1985).

KEYWORDS Yalgoo Dome, Archean, granite-greenstone, sheath fold, Yilgarn Craton

1. INTRODUCTION

1.1. Foreword

The Archean is the second geological eon, extending from 3.8-2.5 Ga. Archean regions contain two types of terranes: low-grade, volcanic-dominated greenstone-granite terranes in the upper crust, and high-grade granulites and gneisses in the mid-lower crust (Tarney & Windley 1981; Windley 1993; Van Kranendonk 2010). The key feature of Archean terranes is greenstone belts separating granite domes. Macgregor (1951), interpreted a granite-greenstone terrane in Zimbabwe as diapiric batholiths being emplaced into a greenstone sequence. Since then, diapirism has become a popular theory to explain granite-greenstone terranes (Myers & Watkins 1985). The Yilgarn Craton has been explained using this theory in studies such as that by Gee (1979). The Yalgoo Dome has been simply described by Muhling and Low (1977) as low-grade metamorphic rocks in curved belts (greenstones), which are intruded by elliptical batholiths. However, the debate as to the formation of the Yalgoo Dome is still unconcluded.

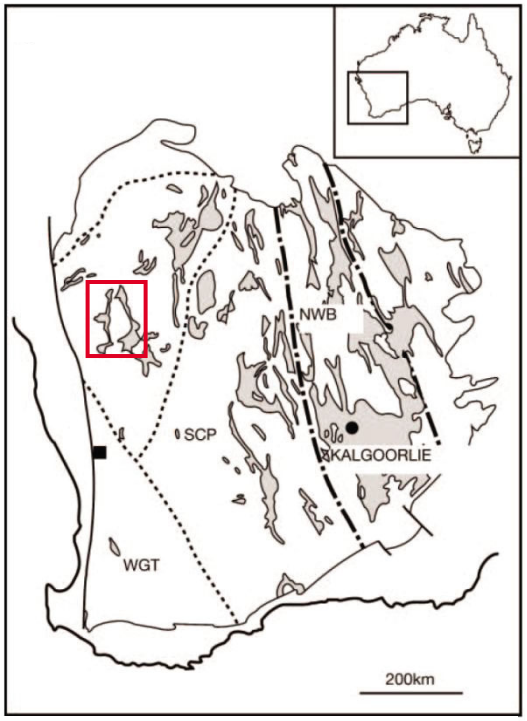

Figure 1 The Yilgarn Craton, Western Australia. The Yalgoo Dome is highlighted by a red box. Figure from Weinberg *et al.* (2005)

1.2. Geographical and Geological Setting

The Yalgoo dome is located just south of the Yalgoo township, in the Murchison Province. The Murchison Province, which makes up part of the Youanmi Terrane,

is an Archean granite-greenstone terrane with several granitoid suites and two greenstone sequences (Watkins & Hickman 1990). In map view, the Yalgoo dome has an elliptical shape, which is elongated north-south and is approximately 95 kilometres long and 50 kilometres wide (Fig. 1).

1.3. Previous Work

There have been limited studies done on the Yalgoo Dome, namely that of Gee *et al.* (1981), Myers and Watkins (1985), Rey *et al.* (1999), and various map sheets published by the Geological Survey of Western Australia. Works from that effort, (Van Kranendonk *et al.* (2013) and Zibra (2012)), are focused on the wider Murchison Province.

Gee *et al.* (1981) proposed that granitoids rose diapirically into the overlying greenstones, due to a density inversion. This produced large antiforms in the granitoids, and synforms in the greenstone belts (Fig. 2).

Myers and Watkins (1985) disagreed with a diapiric emplacement theory for the dome and instead proposed that the structure of the Yalgoo Dome, and the elliptical granitoid intrusions found within it, are dome-and-basin fold interference patterns. They described the deformation history similar to that described by Watkins and Hickman (1990), with D2 consisting of east-west trending folding and D3 consisting of sub-perpendicular, north-northwest to north-northeast trending folding (Fig. 3). They concluded that it is the interference patterns produced by these two deformation phases that produced the Yalgoo Dome.

Rey *et al.* (1999), based on Foley (1997), found that their observations support the diapiric emplacement model of Gee *et al.* (1981), and disagree with Myers and Watkins (1985). However, they also found some differences between the diapiric

model and their observations, namely; sinistral strike-slip movement at the contact between the dome and the greenstones, which suggests a more complex movement than simple vertical displacement, and that the granitoid domes are composed of smaller plutons which were progressively emplaced, rather than in one event. From this, they proposed that the granite-greenstone patterns are formed through progressive incremental strain interference, and that it is the regional finite strain field that is seen in the Murchison Province that resulted in the granitic dome patterns, and was dominated by east-west shortening and north-south extension.

1.4. Aims of this Thesis

This thesis aims at a better understanding of the history of this granite dome and its relation to the greenstone belts surrounding it. In order to do this, our more specific aims are:

- to map in detail specific areas of the dome's core, middle and margin, which are thought to be representative of their corresponding areas across the dome;
- to measure and map the structures in each area;
- to determine a timing relationship between structures in the three areas;
- to determine the nature of the contact and the kinematics at the dome boundary;
- to confirm or reject the fold interference hypothesis (Myers & Watkins 1985), and the progressive incremental strain interference model (Foley 1997)
- to place absolute dating constraints on the occurrence of key events in the dome's history.

In order to see a representation of the entire dome within limited time, I selected three study areas to investigate in detail. Study Area 1 is located within the

migmatitic core of the dome. Study Area 2 is located between the centre and the margin, and is dominated by different granitoid intrusions. Study Area 3 is located at the margin of the dome, on the contact between the dome and the greenstone belt surrounding it. Results from all three areas will be integrated to derive a structural history of the Dome.

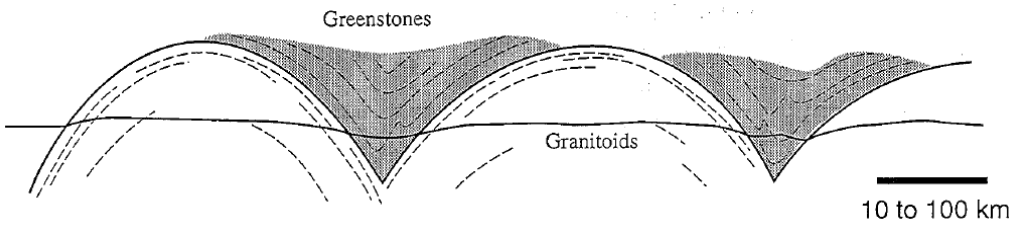

Figure 2 Hypothesis of Gee et al. (1981): Diapiric emplacement of granitoids results in antiforms and synforms within the greenstones. Figure from Foley (1997).

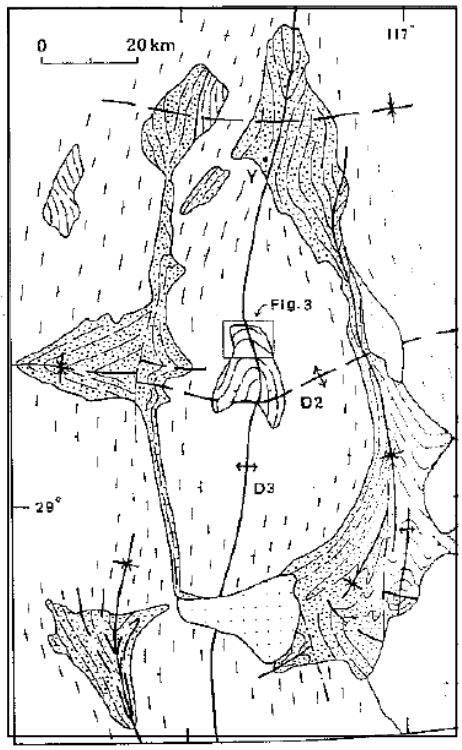

Figure 3 Hypothesis from Myers and Watkins (1985): An E-W trending D2 and a N-S trending D3 folding events produce the fold interference pattern responsible for the dome formation.

2. RESULTS

2.1. Study Area 1

Study Area 1 is located in the core of the dome. This area is dominated by smaller tonalite domes (<200m diameter), each bounded by greenstones which are represented by amphibolite and banded iron formation. This area consisted of three key outcrops, each of which records a different part of the history of the Yalgoo Dome. Figure 4 shows the map produced for the area, and highlights the three key outcrops.

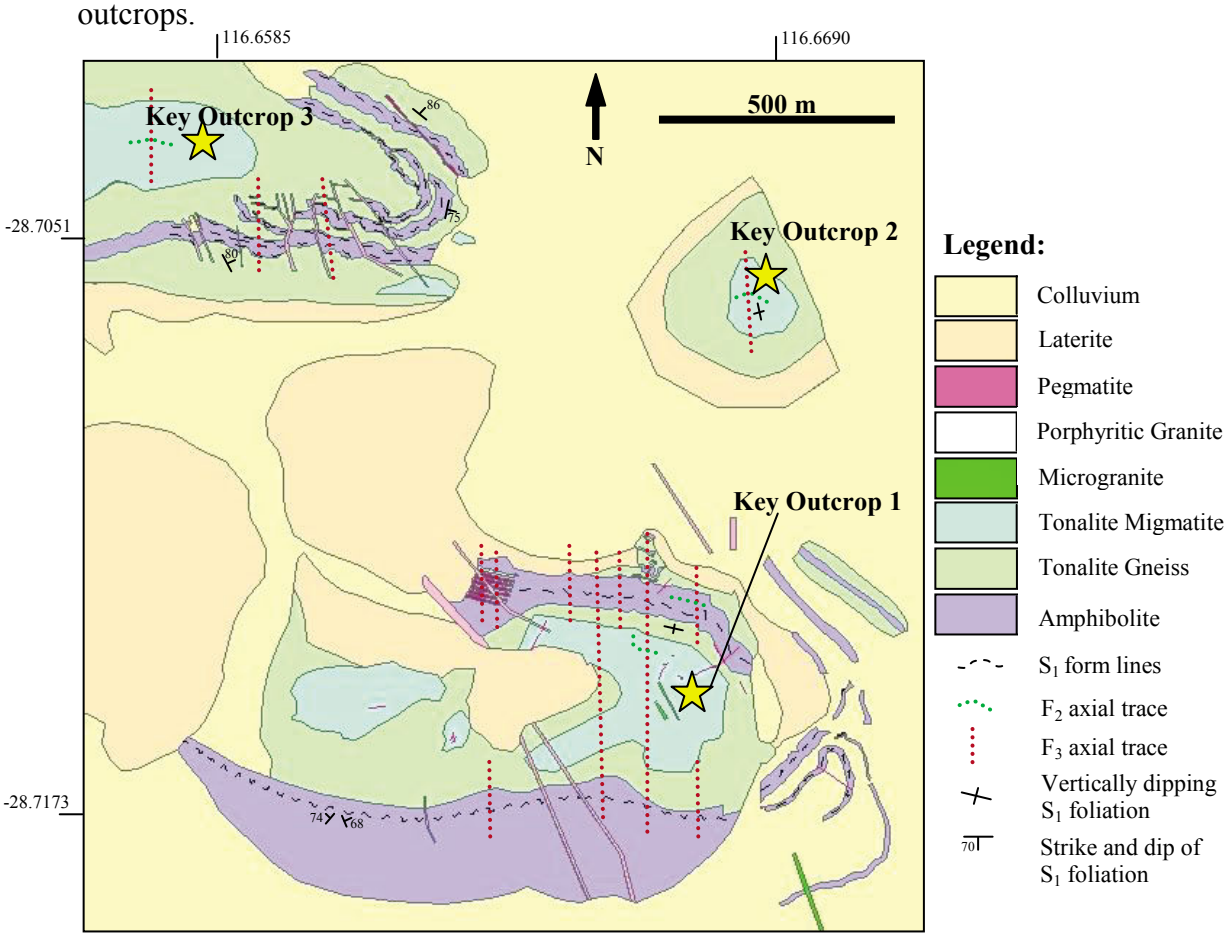

Figure 4 Map produced of Study Area 1. Locations of Key Outcrops 1, 2 and 3 are highlighted. The tonalite domes are bounded by amphibolite and/or banded iron formation (rarer), representative of the greenstone belt.

2.1.1. Rock Types

Study Area 1 is made up of three key rock types, namely a tonalite migmatite and gneiss, and amphibolite. These three are summarised in Table 1, with photomicrographs in Figures 5 and 6. Minor rock types present in the area include pegmatite dykes, Banded Iron Formation (thought to be part of the original greenstone belt, along with the amphibolite), laterite and colluvium. The Banded Iron Formation is generally very weathered, almost to laterite, and therefore is not detailed here.

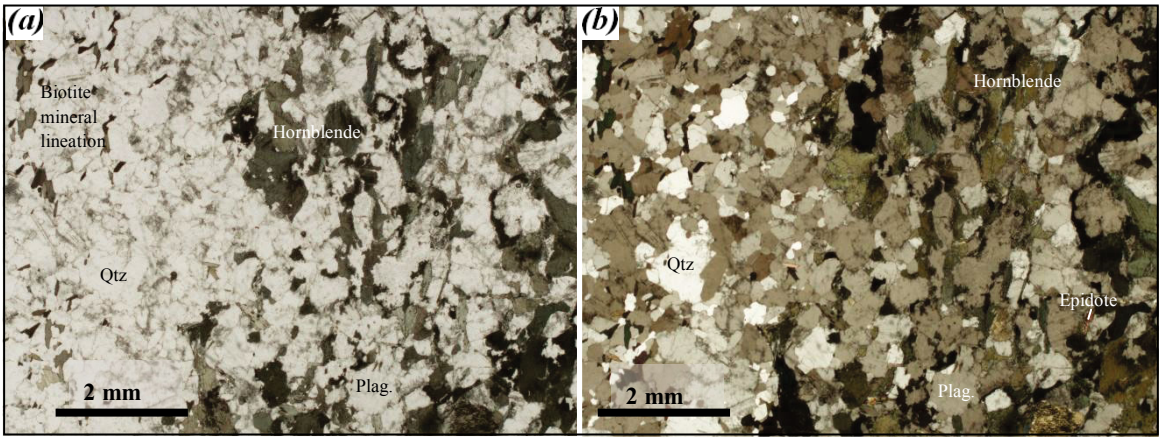

Figure 5 Tonalite migmatite with an amphibolite xenolith; **(a)** photomicrograph in plain polarised light, cut parallel to the lineation, shows steep mineral lineation defined by biotite in host tonalite, with melting and intrusion of the host into the xenolith; (**b)** same with cross-polarised light, highlights the intrusion of the host tonalite into the amphibolite xenolith.

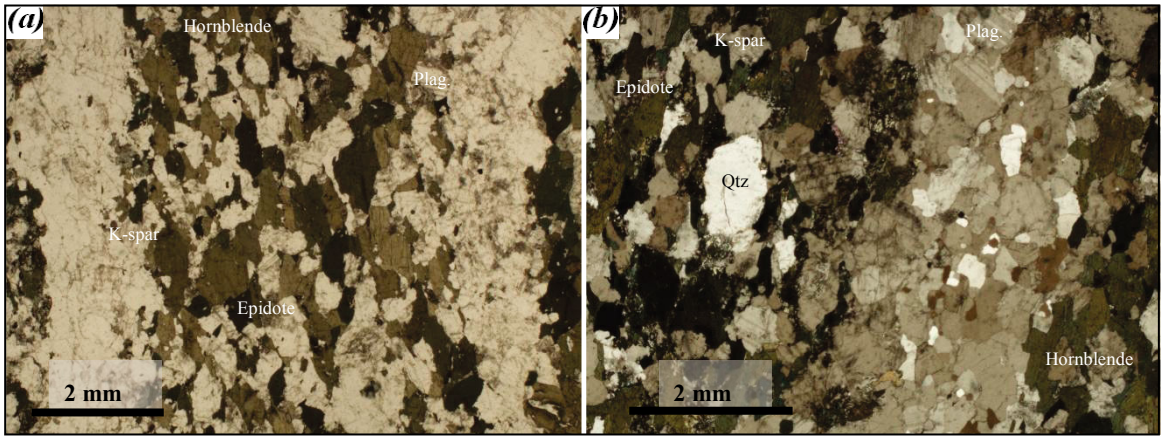

Figure 6 Amphibolite bearing felsic bands, thought to represent a felsic magma; **(a)** photomicrograph in plain polarised light, cut parallel to the lineation, shows steep nature of the felsic bands; **(b)** photomicrograph of same sample as (a), except at a greater zoom and in cross-polarised light, shows the contact between the felsic bands and amphibolite to be defined by the extent of the hornblende, as felsic material is present in both. Also, the hornblende defines the mineral lineation.

Table 1 Petrography and structure of key rock types in Study Area 1

Rock Type	Petrographic comments	Structural comments
Tonalite migmatite	Fine grained (1mm) and is composed of plagioclase (50%), quartz (30%), and biotite (20%). Accessory mineral phases include titanite, apatite and epidote. Leucosomes and melanosomes are both present, however melanosomes are much rarer. Some amphibolite xenoliths are present, however are not common.	Steep mineral lineation defined by biotite alignment. Two key orientations of leucosomes, the first oriented NW-SE, are overprinted and sheared by a the second, oriented N-S. NW-SE leucosomes also include pegmatitic bands, thought to be previous dykes.
Tonalite gneiss	Slightly coarser grained than its migmatitic equivalent (1-2mm), and is composed of plagioclase (45%), quartz (35%) biotite (15%) and K-feldspar (<5%). Pegmatite intrusions common.	Not as deformed as the migmatite, with undulose extinction in quartz grains occasional.
Amphibolite	Fine grained (1mm), composed of hornblende (40%), plagioclase (30%), epidote (15%) and quartz (15%). In situ melting present, with lighter melt bands composed of quartz (45%) and plagioclase (35%) and K-feldspar (15%), with minor hornblende and epidote entrained.	Felsic melt bands are sub-parallel to the metamorphic foliation. Within the melt bands, quartz is relatively undeformed, however within the residual amphibolite, quartz grains frequently display undulose extinction and sub-grain formation.
Porphyritic Granite	Porphyritic texture (K-feldspar porphyroblasts), composed of quartz (30%), K-feldspar (30%), plagioclase (30%), biotite (5%) and muscovite (5%).	Makes up some of the late dykes in the area.
Microgranite	Fine grained (<1mm), composed of quartz (35%), plagioclase (30%), K-feldspar (25%), biotite (5%) and muscovite (5%).	Makes up some of the late dykes in the area.

2.1.2. Key Outcrop 1

Key Outcrop 1 is a large tonalite migmatite platform, that is bounded by amphibolite. Figure 7 shows a representative area of the platform.

The oldest foliation is a metamorphic foliation, which is parallel to leucosomes and pegmatite dykes. This S_1 metamorphic foliation is seen in the amphibolite, however it bears a different orientation. S_1 generally trends NW-SE, however due to it being folded and sheared by later events, it has a variety of orientations (Fig. 8). Leucosomes parallel to the S_1 foliation, have a variety of either sharp and diffuse contacts with the background migmatite (Fig. 7b). This indicates that these leucosomes are both intrusive (sharp boundaries), and in situ melts (diffuse boundaries). Some of the leucosomes are barely visible and traces of felsic crystals can be seen in faint bands.

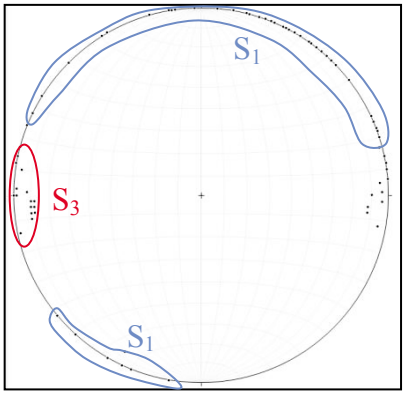

Figure 8 Lower hemisphere equal area stereonet projection showing poles of the planes of foliations in Key Outcrop 1, highlighting the variable S_1 foliation and the N-S S_3 foliation.

S_1 is folded by an F_2 folding event, which consists of upright, gently plunging isoclinal folds with an approximate E-W axial plane (Fig. 7a). This corresponds to the D_2 event of Myers and Watkins (1985). These folds are not common in the outcrop. This may be due to the horizontal nature of the outcrop, and to a possible horizontal-shallow plunging fold axis, making the hinge appear elongate, similar to a limb, in the horizontal plane. Due to the infrequent nature of isoclinal fold closures, and the lack of vertical exposures, measurements were not taken. While the original orientation of the fold cannot be certain due to an S_3 overprint and

potential reorientation, F_2 isoclinal folds are typically E-W trending (drawing on information from Key Outcrop 2).

The S_1 foliation, along with the F_2 isoclinal folds, are folded by F_3 N-S trending folds. These folds have axial planar foliations, S_3, filled with leucosomes. The axial plane acts as slip planes, resulting in shearing along the limbs of the folds. The shearing can be either dextral or sinistral (when viewed in the horizontal plane), and are nearly parallel to each other. This is typical of folding during partial melting (Weinberg & Mark 2008). These S_3 parallel leucosomes again contain a combination of sharp and diffuse boundaries, implying both intrusive and in situ melting. We do not know the vertical component of the shear movement, as there is limited vertical exposure in the outcrop. The S_3 foliation re-orients S_1/S_2 in places, so that it becomes sub-parallel to S_3. Leucosomes in S_3 are regularly spaced, generally with intervals ranging between 20-40 cm (Fig. 7d), and evidence of S_1 being folded in an M-pattern can also be seen. Thus, F_3 folding results from an east-west shortening event and corresponds to the D_3 event of Myers and Watkins (1985). The pegmatite dykes are deformed and sheared in like manner to the leucosomes (Fig. 7c), and so I conclude that these dykes intruded pre-S_3, and pre- or syn-S_1.

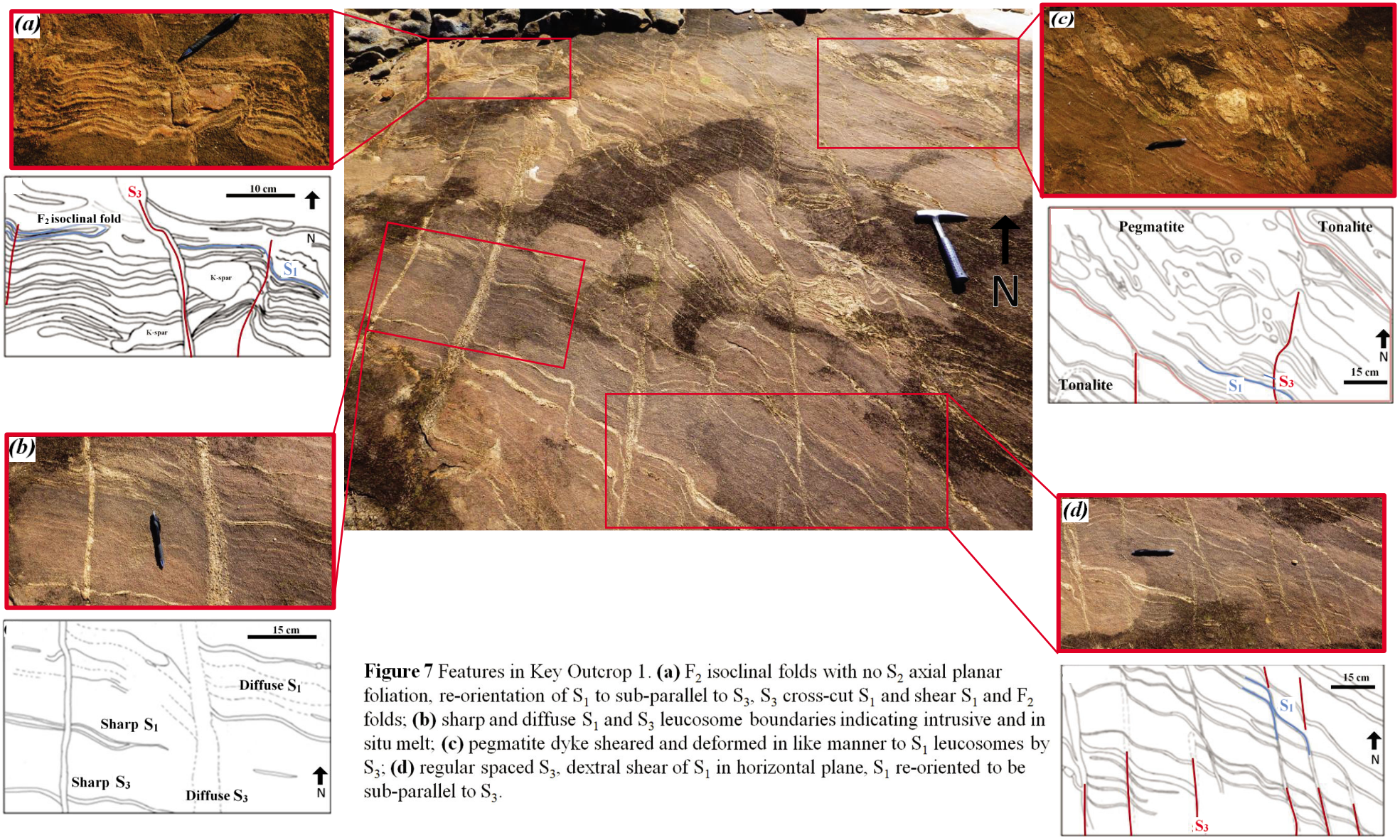

Figure 7 Features in Key Outcrop 1. **(a)** F_2 isoclinal folds with no S_2 axial planar foliation, re-orientation of S_1 to sub-parallel to S_3, S_3 cross-cut S_1 and shear S_1 and F_2 folds; **(b)** sharp and diffuse S_1 and S_3 leucosome boundaries indicating intrusive and in situ melt; **(c)** pegmatite dyke sheared and deformed in like manner to S_1 leucosomes by S_3; **(d)** regular spaced S_3, dextral shear of S_1 in horizontal plane, S_1 re-oriented to be sub-parallel to S_3.

2.1.3. Key Outcrop 2

Key Outcrop 2 is located a few hundred metres N-NE of Key Outcrop 1 and is another tonalite migmatite platform, which is strongly layered with felsic leucocratic bands. The two outcrops have a few important differences.

Like Key Outcrop 1, the early formed leucosomes are sub-parallel to S_1, however they are at a low angle to the S_3 foliation, which is still trends N-S (Fig. 9).

The S_1/S_2 foliation is still dextrally sheared by the S_3 foliation (Fig. 10a). F_2 folds have a non-cylindrical axis, and so can give complex patterns in a horizontal platform (Fig. 10b).

Common in this outcrop are circular, dome-and-basin features (Fig. 10c). The orientation of the long axes of these dome vary from N-S to E-W. Away from D_3 leucosomes, the domes are elongate E-W, however in the vicinity of these N-S leucosomes, the domes trend towards N-S. I interpret the domes away from the D_3 leucosomes to be in their original orientation, as they are in sub-parallel to the F_2 folds seen in Key Outcrop 1 and those away from D_3 leucosomes in Key Outcrop 2 (Fig. 11).

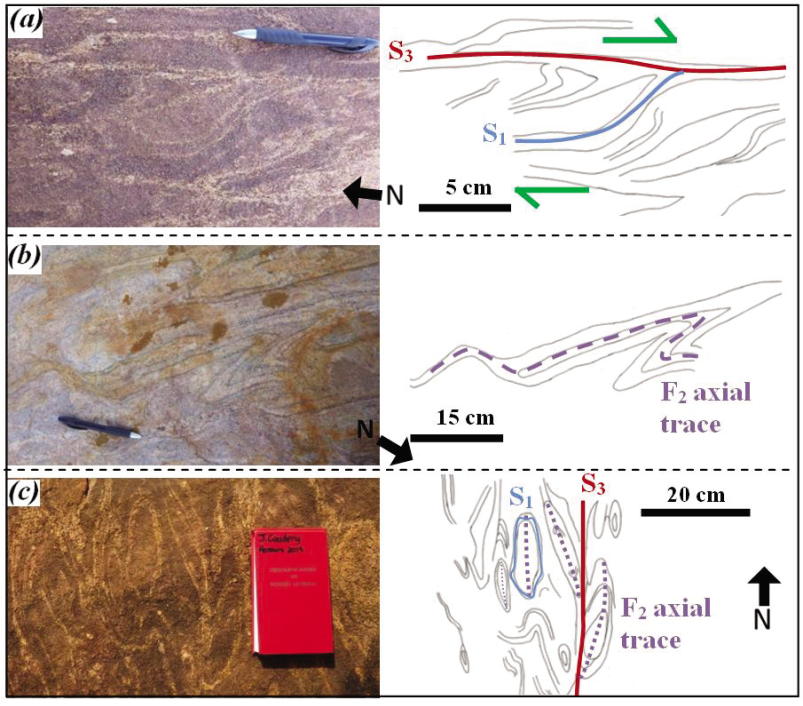

Figure 10 (a) S_1 dextrally sheared by S_3; **(b)** non-cylindrical isoclinal F_2 folding gives complex patterns in a horizontal outcrop; **(c)** Circular, dome-and-basin features are rotated and dragged by S_3.

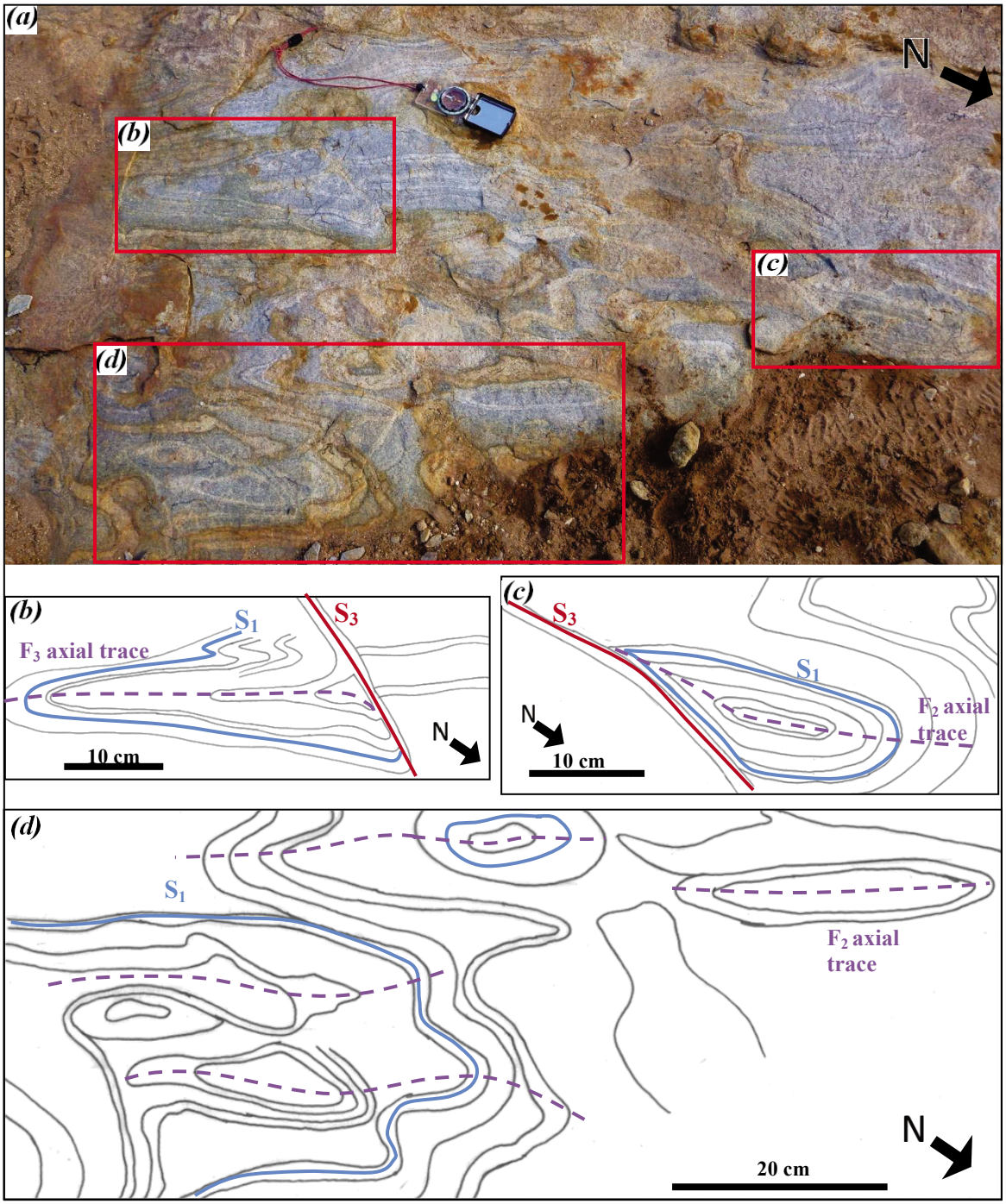

Figure 11 (a) Photograph; **(b)** F_2 folds (D_2 from Myers and Watkins (1985)) deformed by N-S S_3 foliation (D_3 from Myers and Watkins (1985)); **(c)** circular, dome-and-basin feature is dragged by S_3; **(d)** F_2 folds which are not distorted by S_3 share the same axial plane as dome-and-basin features which are not distorted by S_3, indicating they are related to the same event.

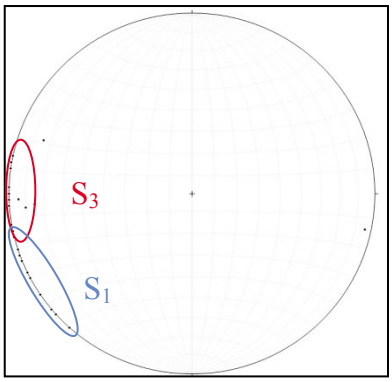

Figure 9 Lower hemisphere equal area stereonet projection plotting poles of the planes of foliations in Key Outcrop 2, highlighting the low angle between S_1 and S_3. Note: S_2 is parallel to S_1.

2.1.4. Key Outcrop 3

Key Outcrop 3 is located a few hundred metres west of 2, and is also a tonalite migmatite platform. In this outcrop, we find that the two axial planes of the F_2 and F_3 folds are at high angles to each other, forming the fold interference patterns described by Myers and Watkins (1985) (Fig. 12). Here, F_2 trends E-W and characterised by isoclinal folds. It is overprinted by open F_3 folds.

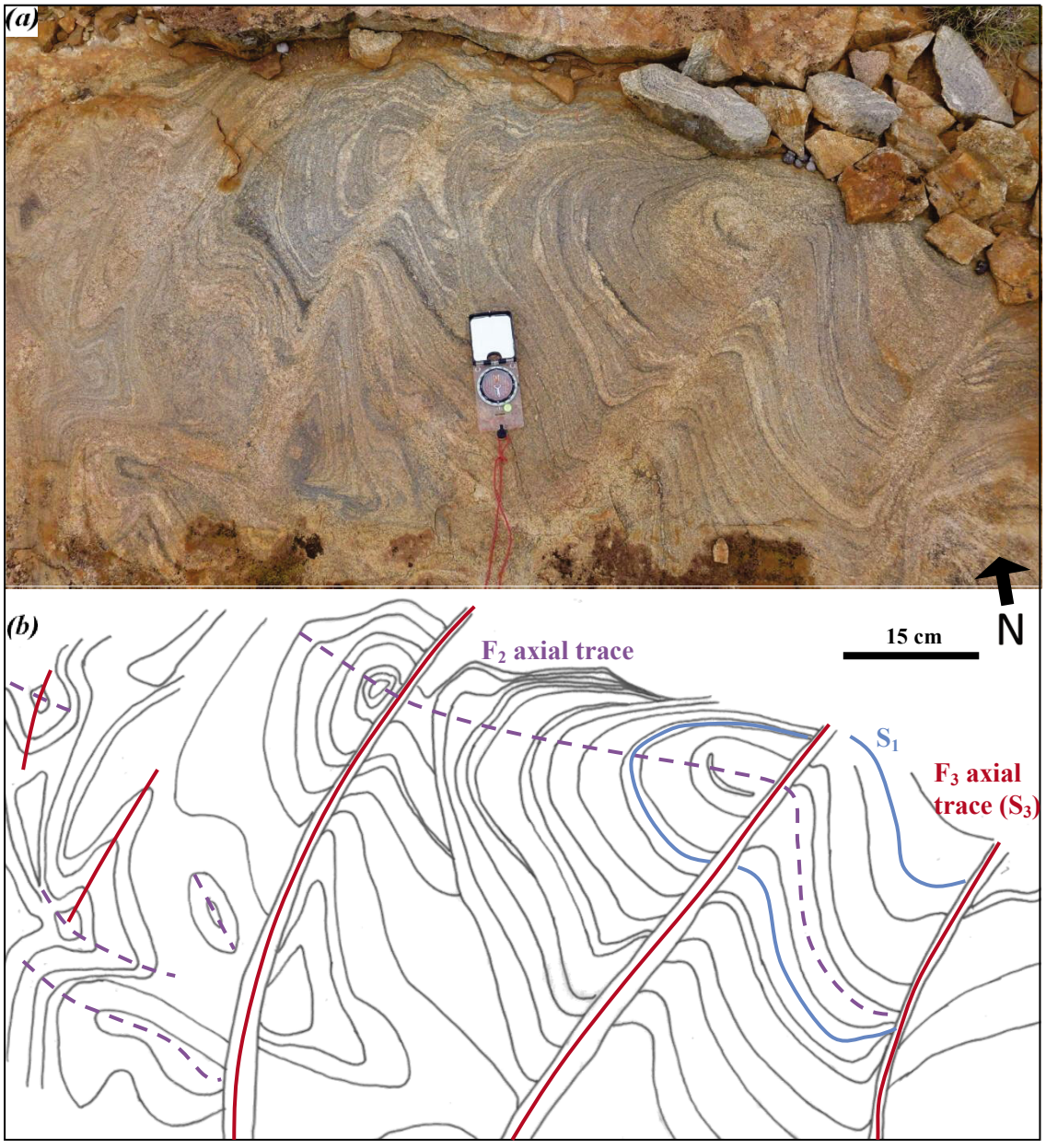

Figure 12 Fold interference patterns produced from $F_2$and F_3 at high angles to each other. Myers and Watkins (1985) described this as D_2 and D_3 respectively; **(a)** photograph; **(b)** sketch of (a).

2.1.5. Amphibolite and Banded Iron Formation

Bounding the tonalite platforms are highly deformed layers of amphibolite and/or banded iron formation (BIF). These layers are country rocks to the tonalite and are likely to represent remnants of the greenstone belt. These define an elliptical feature in the aeromagnetics, and were mapped by Myers and Watkins (1985). Xenoliths of the amphibolite were found within the tonalite migmatite, indicating that the tonalite intruded into the greenstones.

The earliest foliation within the amphibolite is the S_1 metamorphic foliation, which has in situ felsic melt bands sub-parallel. Diffuse N-S leucosomes (parallel to the F_3 axial planar foliation, S_3) cross-cut this foliation (Fig. 13), with in situ melt accumulating in the hinge of F_3 folds, indicating that melting was still occurring during the F_3 event (Fig. 14).

The S_1 foliation follows the margin of the amphibolite, defining the elliptical feature seen in the aeromagnetics, trending E-W, parallel to the main orientation of F_2 folds, with a core of tonalite (Fig. 15a). This foliation is deformed and folded at the scale of metres, with the dominant axial plane being the N-S trending S_3, with a few examples of the E-W trending F_2 folds also observed (Fig. 15). Close investigation of the large E-W trending fold closure, on the east side of the structure, revealed a lack of an S_2 axial plane.

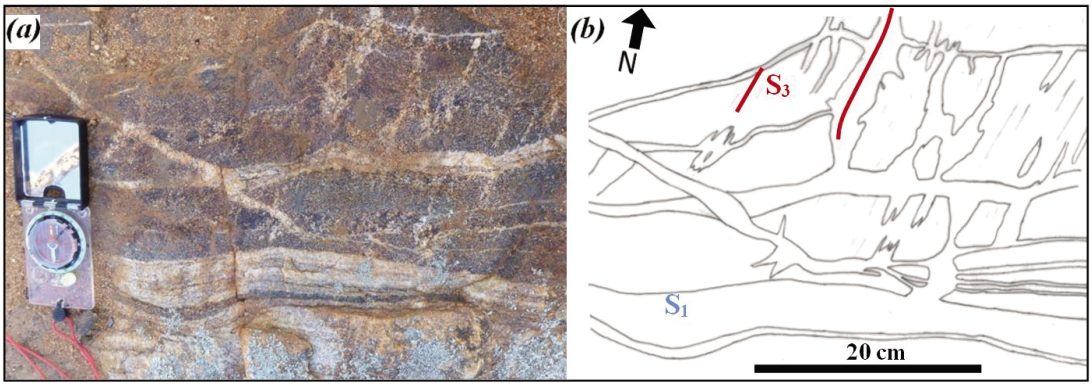

Figure 13 Amphibolite with S_1 melt bands, cross-cut by diffuse S_3 leucosomes **(a)** outcrop photograph; **(b)** sketch of (a).

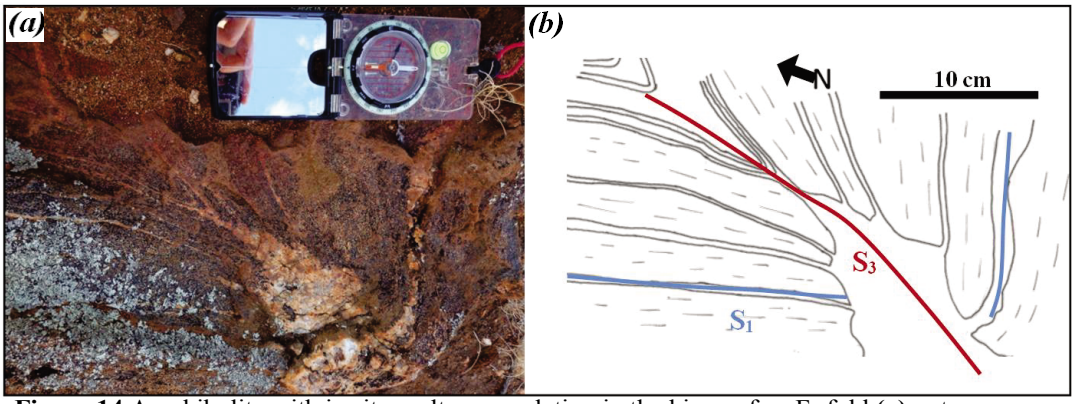

Figure 14 Amphibolite with in situ melt accumulating in the hinge of an F_3 fold **(a)** outcrop photograph; **(b)** sketch of (a).

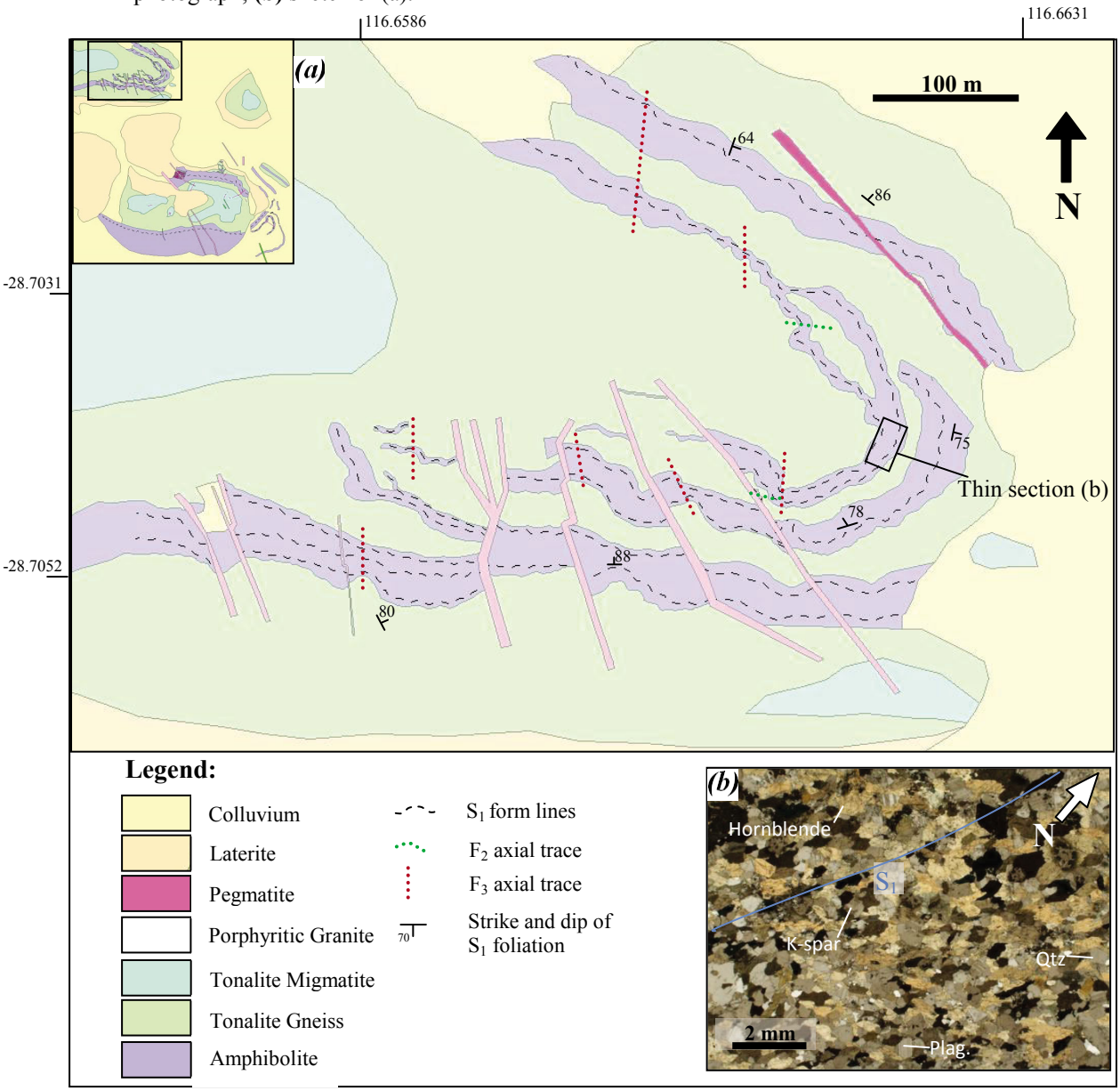

Figure 15 (a) Map of fold closure bounding tonalite migmatite/gneiss dome. S_1 foliation in amphibolite follows around, with porphyritic granite dykes trending 150° cross-cutting the amphibolite. F_2 E-W trending folds and F_3 N-S trending folds present throughout, although the S_2 axial planar foliation is not visible; **(b)** Photomicrograph in cross-polarised light of thin section of amphibolite sample in the hinge of the fold closure, showing a lack of a S_2 foliation. Thin section cut looking down on the S_1 metamorphic foliation from above, as shown in map in (a).
GPS coordinates of thin section: Lat. -28.704364, Long: 116.662700

2.1.6. Late Dykes

There are two generations of late dykes in the three Key Outcrop areas. The older of the two has a general orientation of 150-160^{o}. These are of granitic composition, and are either porphyritic or micro-granular in texture. Schlieren layering is common in dykes found in the migmatite platforms, but was not seen elsewhere. The foliation in the dykes is parallel to dyke orientation, however due to weathering it was impossible to be certain if the foliation was metamorphic or magmatic.

These are cross-cut by an array of younger pegmatite dykes. Their general orientation is 070-110^{o}, but examples of orientations from 020^{o} to 140^{o} were also found.

2.2. Study Area 2

The second study area is located between the migmatitic core and the dome's boundary. The area is dominated by granitic intrusions with a dominant magmatic fabric and tonalite xenoliths oriented parallel to this fabric. The map produced for this area can be seen in Figure 16. The area can be divided into two sections: the south-east and the north-west. The host rocks comprises equigranular and porphyritic granites. These remain unchanged throughout the region. However, xenoliths within these rocks change characteristics from south-east to north-west. Generally speaking, the xenoliths are fewer and in different orientations in the south-east, where in the north-west there are many more xenoliths and they are clearly oriented.

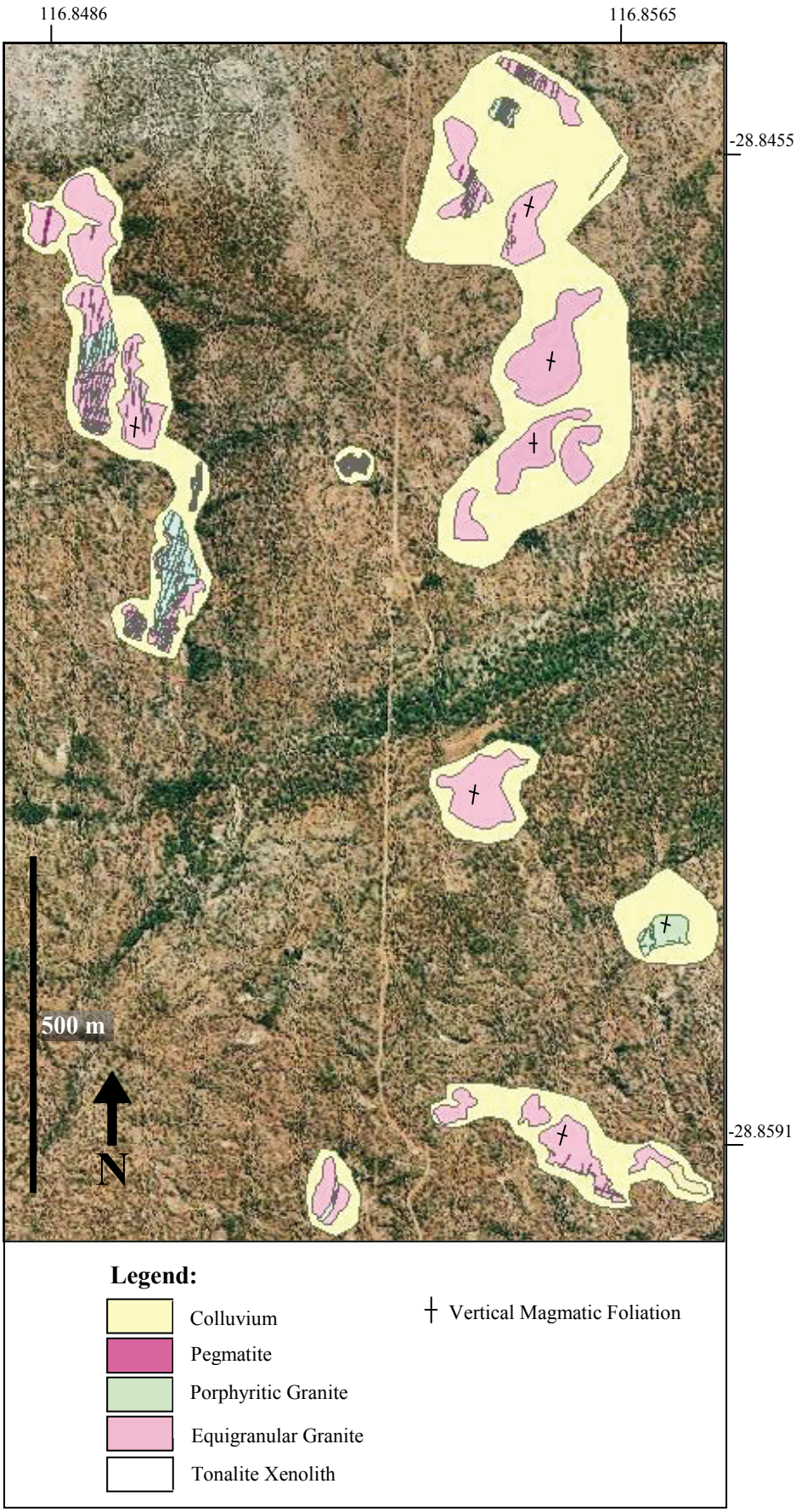

Figure 16 Map produced of Study Area 2 overlaid on an aerial photograph.

2.2.1. Rock Types

Study Area 2 is dominated by two main rock types; equigranular granite and porphyritic granite. Tonalite xenoliths are present in both granites, however the equigranular granite has the highest concentration. Table 2 contains the descriptions of these main rock types shown in Figs. 17 and 18. Pegmatite dykes were also present throughout the region.

Table 2 Petrography and structure of key rock types in Study Area 2

Rock Type:	**Petrographic comments:**	**Structural comments:**
Equigranular Granite (Fig. 17)	Coarse (2-4mm) grained, equigranular texture, composed of quartz (40%), plagioclase (30%), K-feldspar (20%), biotite (5%) and muscovite (5%).	Magmatic foliation, trending NNE. Tonalite xenoliths are elongated NNE. Magmatic foliation flows around the xenoliths.
Porphyritic Granite	Porphyritic texture (K-feldspar porphyroblasts), composed of quartz (30%), K-feldspar (30%), plagioclase (30%), biotite (5%) and muscovite (5%).	Magmatic foliation, trending NNE. Tonalite xenoliths generally aligned parallel to magmatic foliation, however some are at different orientations.
Tonalite xenoliths (Fig. 18)	Fine grained (>1mm), composed of quartz (45%), plagioclase (40%), biotite (10%), k-spar (5%) and muscovite (5%). Some xenoliths have biotite rich bands. Biotite is commonly chloritised, and sericitisation of plagioclase is frequent. Some xenoliths can be described as leucotonalites.	Highly deformed, with a strong metamorphic foliation trending parallel to the strike of the xenolith, which is parallel to the magmatic foliation of the host granitoid.

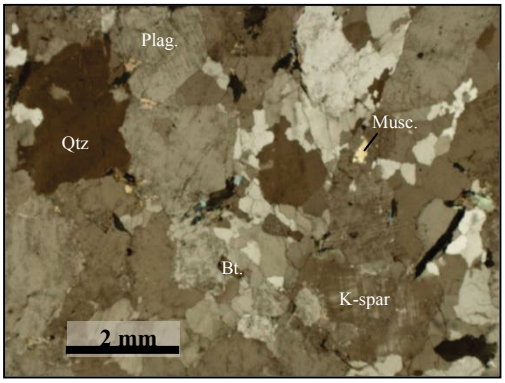

Figure 17 Photomicrograph in cross-polarised light, of equigranular granite.

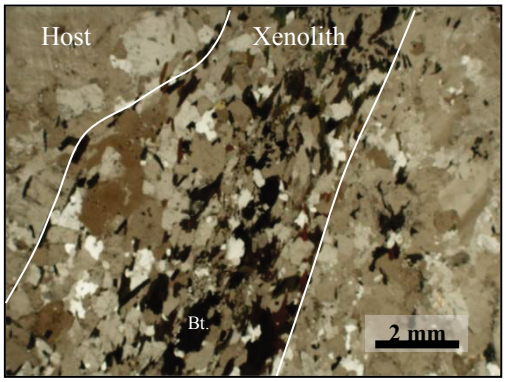

Figure 18 Photomicrograph in cross-polarised light, cut perpendicular to the foliation, down dip, of a tonalite xenolith in the host equigranular granite. The xenolith has a sharp boundary on the right side, and a curved, diffuse boundary on the left.

2.2.2. Study Area 2 South-East

The south-eastern section of Study Area 2 is dominated by platforms of equigranular granite, with a few platforms of porphyritic granite. Tonalite xenoliths are found within both of these granitoids.

The larger xenoliths, which are more than 10 m long, are generally aligned N-S to NE-SW, but the orientation of the smaller xenoliths appeared to lack a preferential alignment, as seen in the porphyritic granite platform in Figure 19.

The xenoliths are generally elongated, less than one metre wide, and up to tens of metres long. They have a sharp contact with the host rock on one boundary, and a gradual contact on the other, with evidence of re-melting and melt penetration. Interfingering of the host rock and the xenolith is common. Examples with irregular, lobate boundaries were also found, along with boudinaging with box-shaped boudins dominant (Fig. 20).

The host granitoids have a preferential orientation of K-feldspar, indicative of a magmatic fabric (Paterson *et al.* 1989). The magmatic foliation trends NNE and flows around the xenoliths (Fig. 20c).

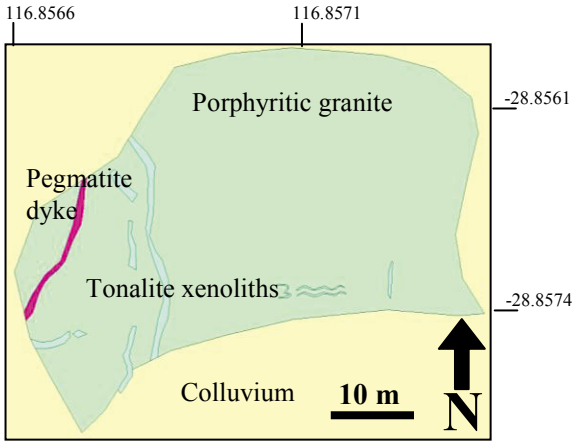

Figure 19 SE outcrop comprised dominantly of porphyritic granite, where larger tonalite xenoliths are aligned N-S, and the smaller xenoliths lack a preferred orientation.

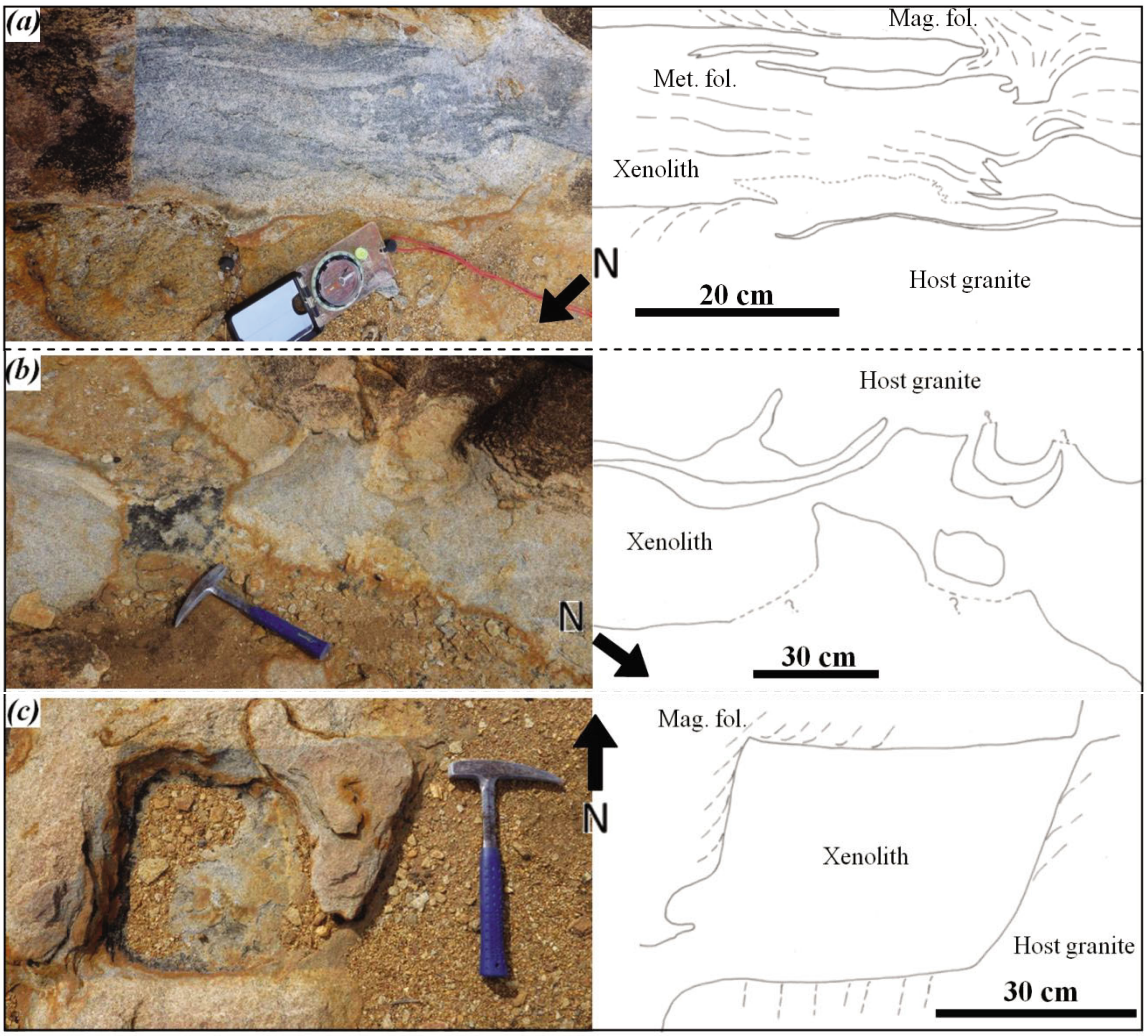

Figure 20 Key features of the tonalite xenoliths in the South-East region. **(a)** Sharp contact on western margin, with a gradual contact on the eastern margin, along with inter-fingering with host rock present; **(b)** irregular, lobate margins of xenolith; **(c)** box-shaped boudins, with host rock magmatic foliation flowing around the xenolith.

2.2.3. Study Area 2 North-West

The north-western region of Study Area 2 is similar to the south-eastern region, with one key difference: the equigranular granite platforms have higher concentration of xenoliths (Fig. 21).

There is evidence of the host granite penetrating the xenolith, and also of the xenolith being melted and penetrating into the granite (Fig. 22). The xenolith is mostly intact, but is eroded by the host granite at its margins. In the centre, it is broken up and separated, but dominantly parallel to the magmatic foliation (Fig

23). Some separation perpendicular to the magmatic foliation occurs, but the split and movement is only on the order of centimetres.

The xenolith can be traced to be over 300m long, and with interpretation through cover, could be over a kilometre long, with various offshoots and interfingering occurring with the host granite. The map in Figure 16 shows the outcropping of the xenolith, and demonstrates that what we see in the outcrop scale, could be similar to what is seen on the larger scale.

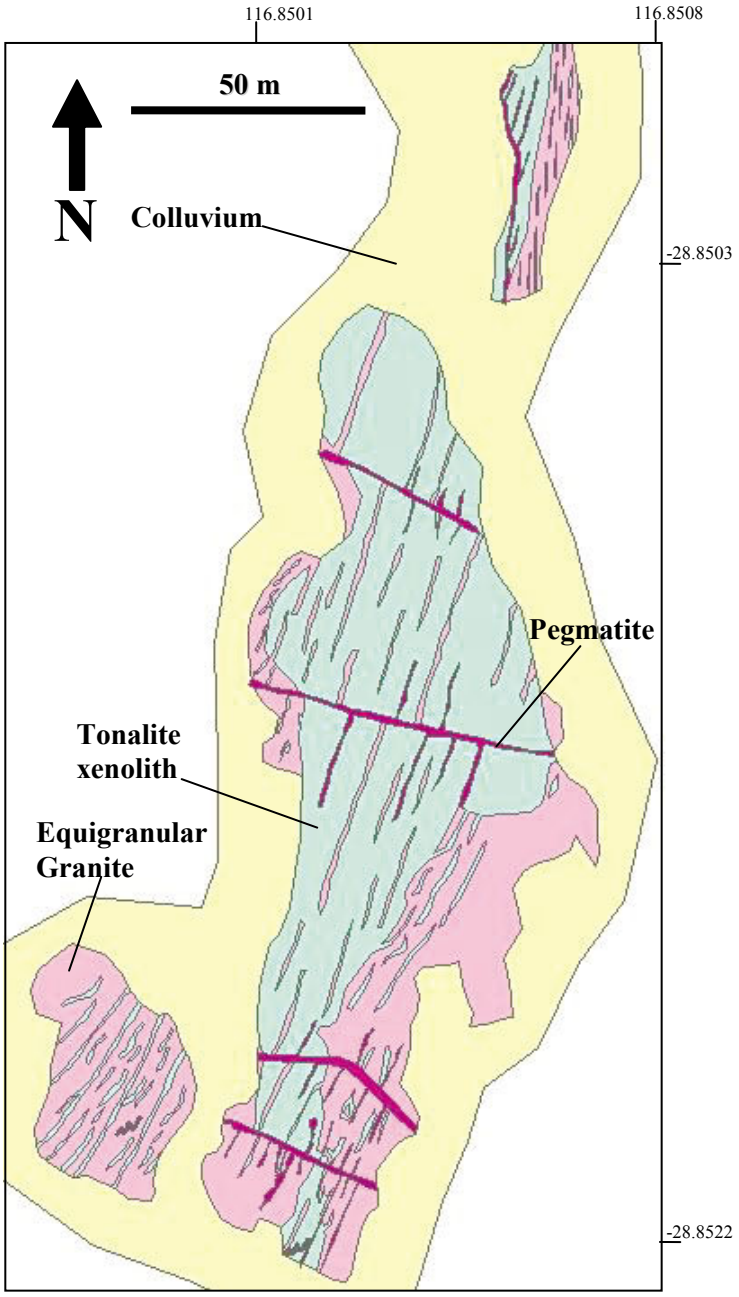

Figure 21 Part of the map of the equigranular granite platform . The large tonalite xenolith has been broken up and entrained in the host granite.

Pegmatite dykes also occur in the region, with the general trend being 090-130°. The dykes are younger, but they have been melted, with pegmatitic melt migrating preferentially along the magmatic foliation of the host granite (Fig. 21). The magmatic foliation trends NNE, with the metamorphic foliation of the xenoliths sub-parallel to it (Fig. 24).

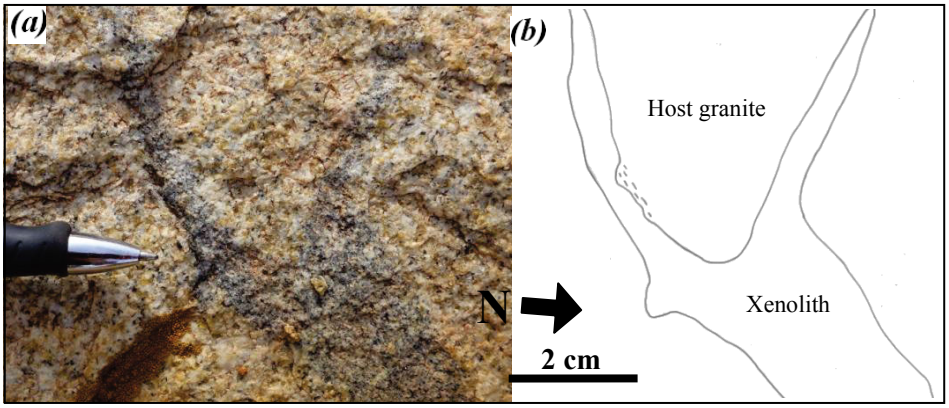

Figure 22 Tonalite xenolith has penetrate the host granite. **(a)** outcrop photograph; **(b)** sketch of (a).

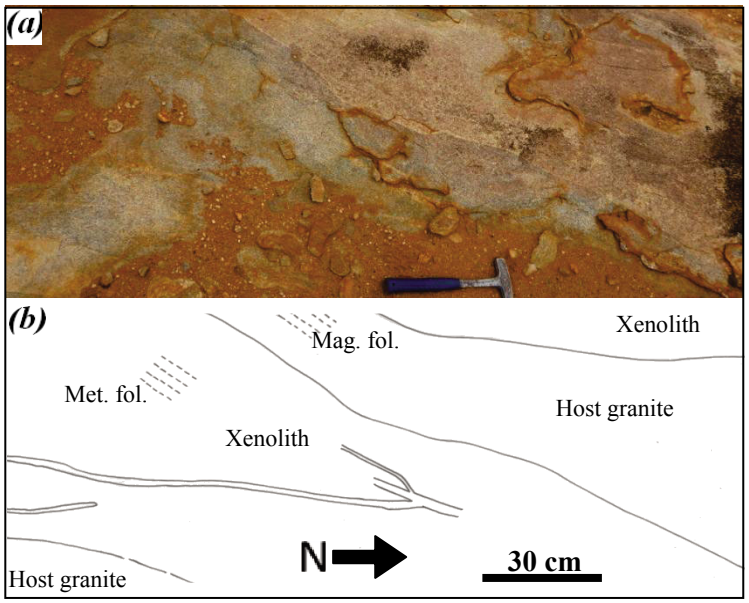

Figure 23 The tonalite xenolith is broken along the dominant magmatic foliation. Compare with Fig. 22. **(a)** outcrop photograph. **(b)** sketch of (a).

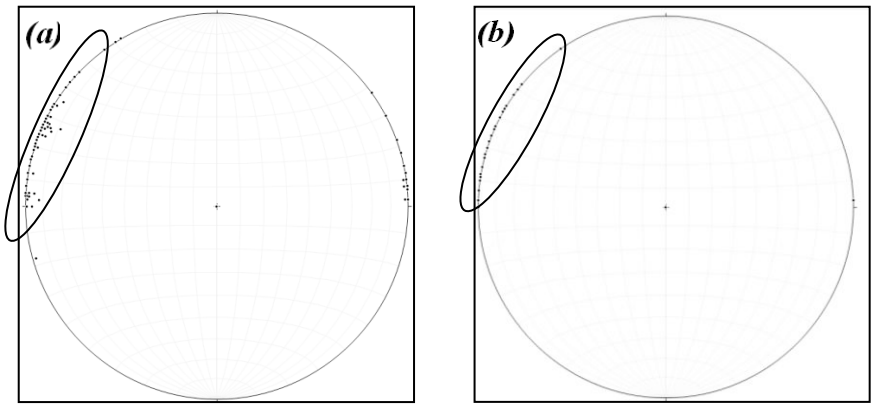

Figure 24 Lower hemisphere equal area stereonet projection plotting the poles to the planes of the foliations; **(a)** magmatic foliation in the host granites trending NNE; **(b)** metamorphic foliation in the tonalite xenoliths also trending NNE.

2.3. Study Area 3

The third study area is located on the margin of the dome, on the contact between the dome and the surrounding greenstone belt. This is an ideal area to detail the nature of the deformation at the margin of the dome.

2.3.1. Rock Types

The two main rock suites in the area are the granitoids from the dome, and highly deformed schists, amphibolite and intrusives from the greenstone belt. The granitoids are highly deformed and are muscovite rich. The rock types of Study Area 3 are summarised in Table 3.

Table 3 Petrography and structure of key rock types in Study Area 3

Rock Type:	**Petrographic comments:**	**Structural comments:**
Granitic gneiss	Fine grained (<1mm), composed of quartz (40%), muscovite (20%),plagioclase (10%), K-feldspar (10%) and biotite (10%).	Highly deformed, recrystallised quartz ribbons. Micas define lineation.
Dolerite, Garnet-bearing dolerite, plagioclase-rich leucogabbro.	There are three variations of dolerite in the area. The first, is fine-grained and composed of plagioclase and pyroxene. The second is similar to the first, however it is has garnet porphyroblasts (2mm). The last, is plagioclase-rich and coarse grained (10mm), with large crystals of plagioclase and clinopyroxene.	Highly deformed, with garnet porphyroblast rotation and sigma clasts indicating kinematics.
Chlorite schist	Fine-grained (<0.5mm), composed of chlorite (50%), quartz (40%), opaque minerals (10%).	Quartz is very fine grained (<0.25mm), and forms clusters which look like clasts in hand specimen. Chlorite is deformed around these clusters of recrystallised quartz.
Chlorite-garnet schist	Fine grained (<0.5mm), porphyroblastic texture with garnet porphyroblasts (10%), composed of chlorite (50%), quartz (40%), garnet (10%).	Garnet porphyroblasts have been broken apart perpendicular to the shear planes, with quartz recrystallising in the cracks. High deformation has lead to porphyroblast rotation and sigma clasts, and a late crenulation cleavage has developed in the mica matrix.

Amphibolite	Fine-grained (1mm), composed of hornblende, plagioclase, epidote and quartz.	Strong metamorphic foliation trending NNE, dipping west.

2.3.2. Kinematics

In the third study area, we traversed the boundary of the dome and produced a map and cross section. The dominant metamorphic foliation of the area trends north to north-east, dipping west to north-west at 50-80^{o} (Fig. 25). Figure 26 shows the map and cross-section produced.

The contact contains several smaller interlayered units of both greenstones and granite. Due to this, the precise boundary of the dome is uncertain, and so an approximate region for the boundary is given in the cross-section instead. The 3D geometry of these units is poorly understood, and so the cross-section is kept intentionally simplified.

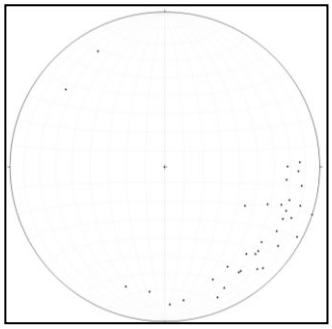

Figure 25 Lower hemisphere equal area stereonet projection plotting poles to the planes of the metamorphic foliation in Study Area 3 with general strike of NNE and dip of 50-80^{o} WNW.

A number of thin sections across the cross-section and from different units, were made in order to determine the kinematics of the dome relative to the greenstone belt. The majority of the thin sections display dome-up, or normal, movement kinematics (Fig. 27). However there were two thin sections which gave reverse sense, or dome-down (Fig. 28). A late crenulation cleavage was observed in the weakest layers the field (Fig. 29) and can be seen in thin section (Fig. 28a).

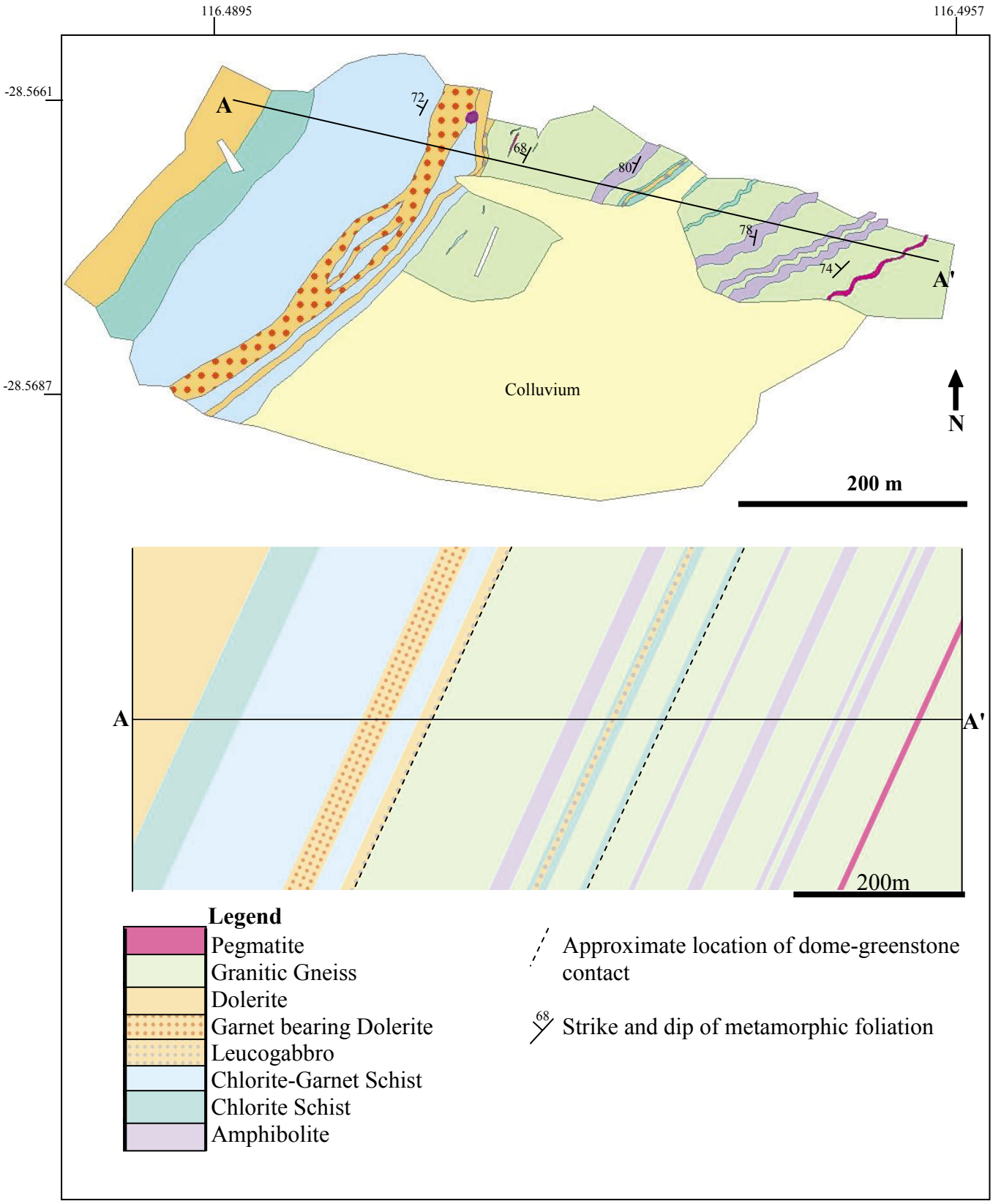

Figure 26 Map and cross-section of Study Area 3. Note: corrections for creep and slump effects on the units on the west side of the section (chlorite schist and dolerite) have been made. In the field they are found to be dipping towards the east at approximately 50°, however we assume they were originally at similar, westward dipping orientations to their counterparts further to the east.

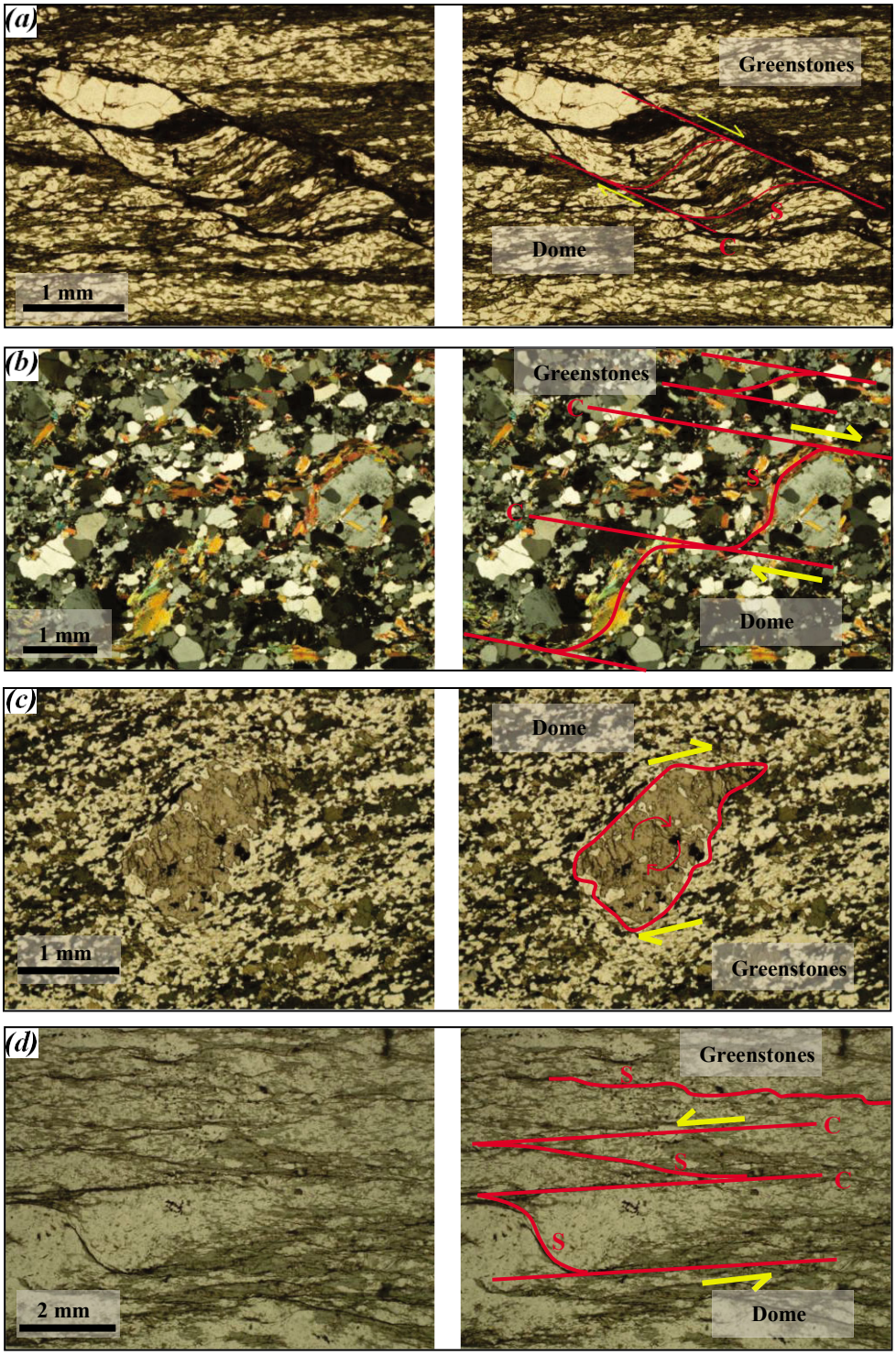

Figure 27 Photomicrographs displaying dome-up (normal movement) kinematics and their interpretations (right column). All sections are cut perpendicular to the foliation, parallel to the lineation (assumed down dip); **(a)** chlorite schist displaying S-C planes, photomicrograph is in plane polarised light; **(b)** granitic gneiss displaying S-C planes, with the S planes defined by muscovite stepping and quartz ribbons, photomicrograph is in cross-polarised light; **(c)** garnet bearing dolerite, displaying sigma-shaped garnet porphyroblasts indicating rotation, plane polarised light; **(d)** chlorite schist displaying S-C planes, plane polarised light.

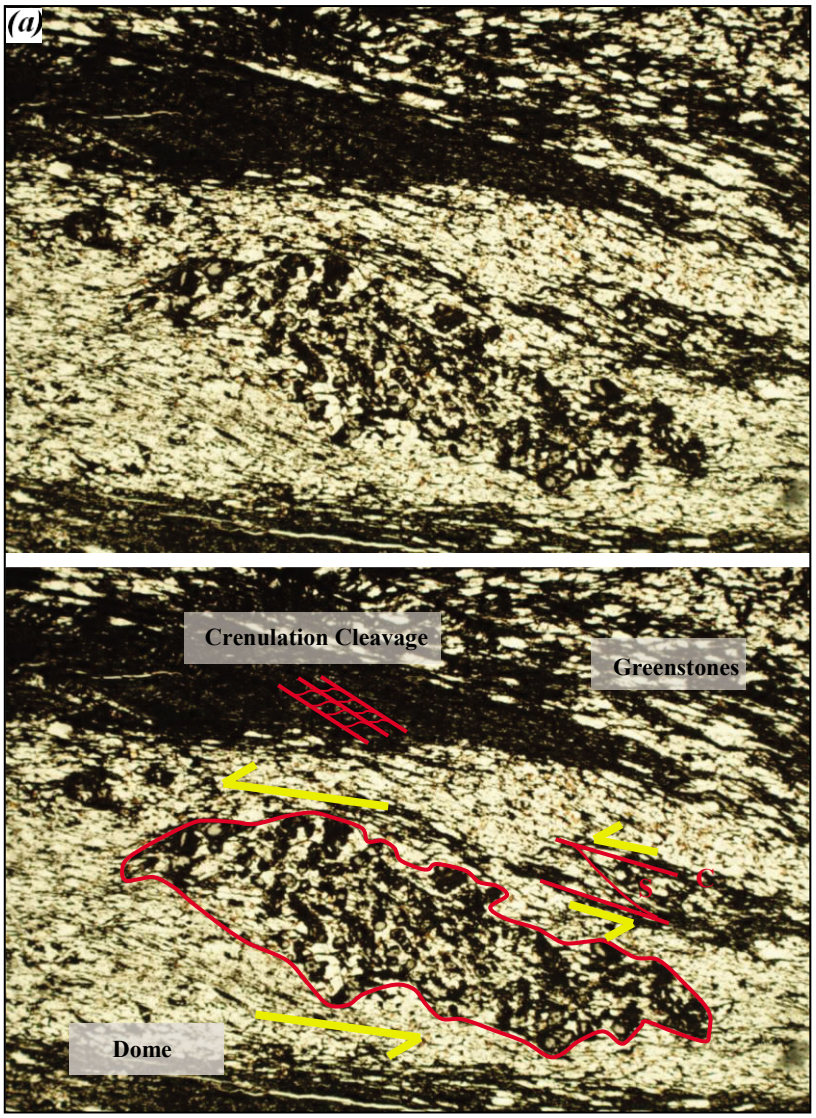

Figure 28 Thin sections of a chlorite-garnet schist displaying reverse kinematics. This schist also shows the late crenulation cleavage.

(a) Photomicrograph and interpration showing garnet porphyroblast rotation, along with limited S-C planes in the surrounding chlorite matrix. A late crenulation cleavage can be seen in the chlorite matrix above the porphyroblast.

(b) The same sample in hand specimen, with sigma porphyroblasts indicating the reverse-sense kinematics.

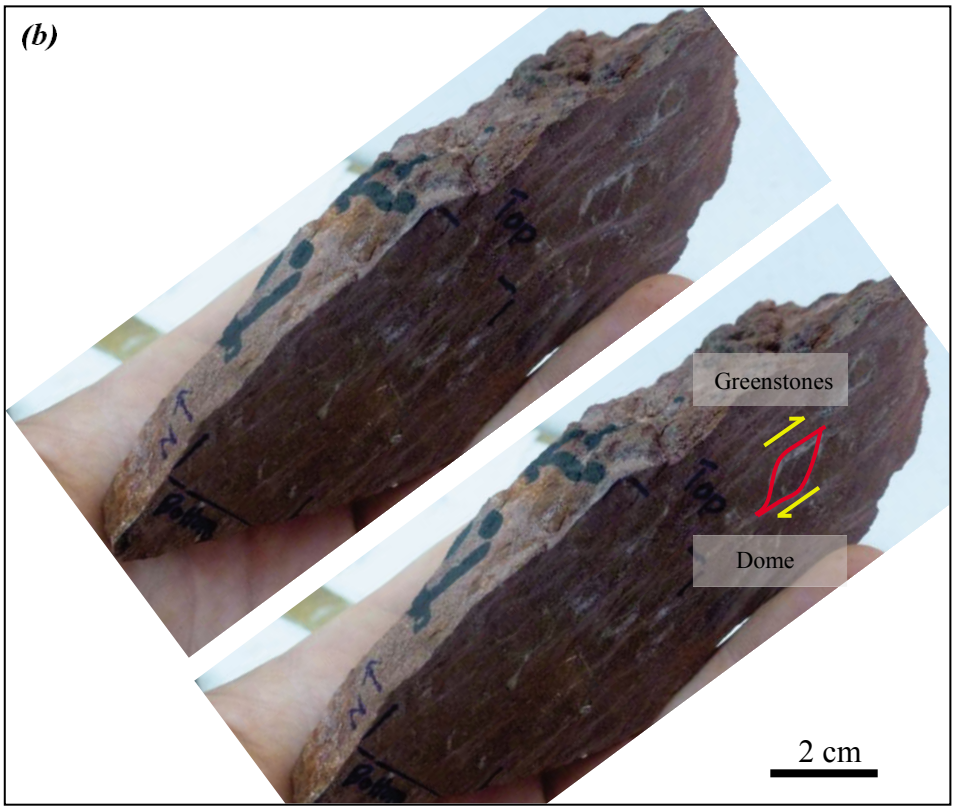

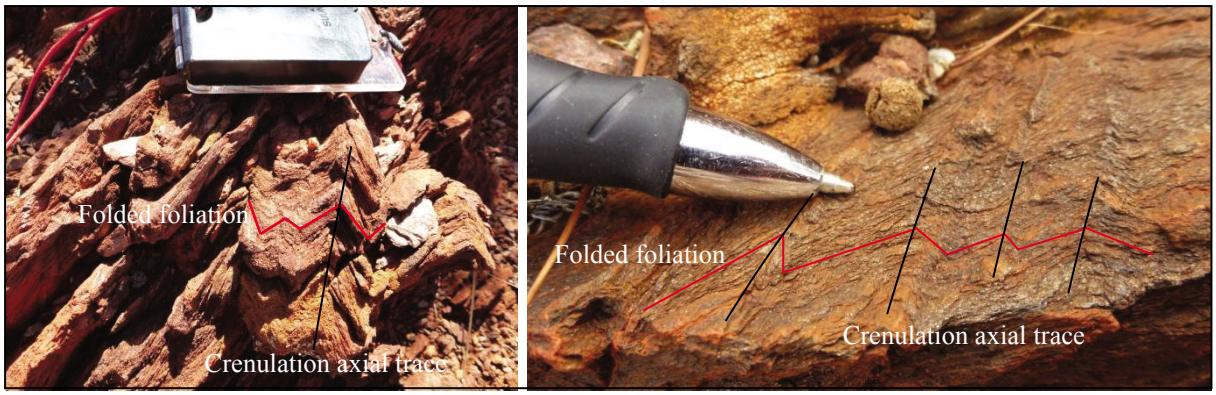

Figure 29 Chlorite-garnet schist displaying a crenulation cleavage with an axial plane at 165/70 W and a fold axis of 42→345.

2.4. SHRIMP Dating

Three samples were analysed for dating but unfortunately the results arrived two days before the deadline for submittal of this work. Full details of the dating results can be found in Appendix C, and are summarised in Table 4 below.

Table 4 Summary of SHRIMP results

Sample	**Rock Type**	**Location**	**Result**
209689	Tonalite Migmatite	Study Area 1 Lat: -28.714629 Long: 116.667277	2960±10 Ma. Interpreted as the magmatic crystallisation age of the tonalite protolith.
155858	Porphyritic Granite	Study Area 2 Lat:- 28.786148 Long: 116.809026	2752±13 Ma. Interpreted as the magmatic crystallisation age of the granite.
212003	Late Granite Dyke	Study Area 1 Lat: -28.530448 Long: 116.768063	No zircons.

It is uncertain whether or not the magmatic crystallisation age of the porphyritic granite from Study Area 2, is representative of the majority of granites in the area or not.

3. DISCUSSION

This work looked at three study areas. Study Area 1 is the oldest, with tonalite intrusions into amphibolite country rock. Study Area 2 contained later granitoid intrusions with a magmatic fabric, which entrained xenoliths of the older tonalite from Study Area 1. Study Area 3 contained the same granites as 2, however they have a solid state overprint, which is younger than the magmatic foliation.

3.1. Discussion of Study Area 1

Each of the three outcrops of Study Area 1 provide a different part of the history. In Key Outcrop 1, tonalite intruded into the greenstones, evidenced by xenoliths. The earliest foliation (S_1) found in the area is the metamorphic foliation with sub-parallel leucosomes or felsic melt bands in the tonalite and amphibolite respectively. Examples of both in situ and intrusive leucosomes exist, and is likely that the intrusive leucosomes melted from the same package of rock, just at a lower depth. Pegmatite dykes were also found to be a part of the S_1 foliation and probably intruded pre- or syn- melting. Similar pegmatite dykes were found in greater abundance in Key Outcrop 2, and rotated to be sub-parallel to S_1. This indicates that the pre-S_1 history is more complicated than can be derived.

The S_1 foliation was folded isoclinally, forming F_2 folds, which were observed both in the tonalite and amphibolite packages. The F_2 event also included sheath folding, as found in Key Outcrop 2, evidenced by sub-parallel E-W axial traces. This is important because it indicates that D2 gave rise to E-W trending non-cylindrical folds that could potentially explain the origin of the domes. Key Outcrop 2 shows that the S_3 foliation overprints the small scale dome-and-basin features, and so cannot possibly be involved in their formation. This contrasts

with the interpretation by Myers and Watkins (1985), who interpreted the dome-and-basin structures to have formed as a result of fold interference, like that observed in Key Outcrop 3. This outcrop showed the N-S F_3 axial plane and the E-W F_2 axial plane to be at high angles to each other, forming domal patterns in a horizontal platform. The development of D_2 E-W trending sheath folds suggest the possibility that the E-W trending domes mapped at the scale of hundreds of metres (Figs. 4 and 15) result from this event, similar to that proposed by Foley (1997). The limbs of these D_2 domes are folded by metre scale N-S trending folds, but these post-date dome formation and are not the cause of it.

The S_3 foliation was found to be an axial planar foliation of an F_3 folding event, which occurred due to east-west compression. Melting was still occurring at this time, and accumulated along the axial planes and hinge zones of F_3 folds, as well as migrating preferentially along the N-S S_3 axial planar foliation. This folding event caused both dextral and sinistral shearing in the horizontal plane of the previous foliations and folds, with S_3 as slip planes (Weinberg & Mark 2008). Dextral shearing was seen in Study Area 1 because it was located on the eastern limb of a larger scale F_3 anitform. If we travelled west onto the opposite limb, the shearing would be sinistral. Comments cannot be made on the 3D aspect of the shearing , due to limited vertical exposure. The earlier foliations and folds where rotated, re-orientated, truncated and sheared by the S_3 foliation.

Two generations of late dykes were observed, with pegmatite dykes being the most recent. The granitic dykes, orientated at around 150^{o}, were found throughout the area and are most likely related to the granites in Study Area 2.

3.2. Discussion of Study Area 2

The second study area is made up of various granitoid intrusions, with tonalite xenoliths throughout the region.

In the south-east area, several outcrop scale or smaller xenoliths where observed, but in the north-west area, at least one large (>300m) xenolith was observed, demonstrating similar characteristics to the small scale ones; such as interfingering with the host granite, boudinage, alignment along magmatic foliation, and melt penetration into, and by, the host granite. I suggest that the smaller xenoliths are offshoots and interfingers of the large xenolith. However, the xenoliths in the south-east are not connected to the large xenolith and were most likely entrained as separate xenoliths. Evidence for this is the small distance which the granite flowed after xenolith separation (on the order of centimetres), and the xenoliths in the south-east are several hundred metres away. I suggest that the tonalite xenoliths are actually from the tonalite migmatitic core of the dome, and were entrained by the younger intruding granites. At least one of the xenoliths entrained was over 300 metres long, most likely over 1 kilometre long, as evidenced by the alignment of the xenoliths seen in the maps. However, in the scale of the dome, this is not of significant size, and there could well be many more of this size xenoliths or larger, in other locations around the dome. The intruding granites broke the large xenolith apart in two ways: through melt flow breaking perpendicular to the flow direction, and also from melt penetration parallel to the foliation in the xenoliths. Also, due to the heat from the intruding granites, the xenolith began to melt and penetrate into the host rock.

Younger pegmatite dykes intruded while the host granite was still hot. Melt from the pegmatite intrusions migrated along the magmatic foliation of the host.

Study Area 2 records none of the events recorded in Study Area 1. We postulate that the porphyritic granite dykes, trending at 150^{o} in Study Area 1, is part of the same generation as the porphyritic granite seen in Study Area 2. This is because of their similarity and their absence in cross-cutting granitoids in Study Area 2.

The latest pegmatite dykes are in similar orientations in both Study Areas (approximately E-W), and could be one and the same event.

3.3. Discussion of Study Area 3

The dome-greenstone contact investigated in Study Area 3 is a sheared intrusive contact, evidenced by the smaller interfingered units of granite and greenstone. These units are granite dykes in the greenstones, and greenstone xenoliths in the dome margins. However, the 3D geometry of these dykes and xenoliths are poorly understood.

The kinematics of the contact was determined by several shear sense indicators, most of which indicated dome-up, or normal movement, kinematics. However, some samples gave opposing results. In the area there is a late crenulation cleavage. This is only observed in the weakest units, such as the chlorite-garnet schist, suggesting it was a minor and local event. However, this may be an important local feature.

There are three possible models for the kinematics of the dome relative to the greenstones. The first, which is the currently accepted model, is that the dome came up relative to the greenstones (normal movement) (Gee *et al.* 1981). The second, is

that the dome is older and the greenstones were thrust up onto the dome, giving dome down (reverse) movement. The third, is that there were two events, one with normal movement and another with reverse. No overprinting relationship of the two kinematics could be determined.

There were two samples displaying reverse kinematics; the chlorite-garnet schist (which also recorded the late crenulation cleavage) and the granitic gneiss (which does not record the crenulation cleavage). It seems most likely that doming occurred with normal movement relative to the greenstones, with the late crenulation cleavage re-rotating some of the porphyroblasts. Johnson *et al.* (2006) found that a late crenulation cleavage can rotate porphyroblasts into different orientations (Fig. 30). The shear sense can still be determined in the remnant foliation within the porphyroblasts, however this could not be determined as the garnet porphyroblasts had been pulled apart perpendicular to the direction of movement. The granitic gneiss also displayed normal kinematics, and may have been further complicated through quartz recrystallising into clusters, causing the muscovite (which defines the S planes), to be rotated around the quartz.

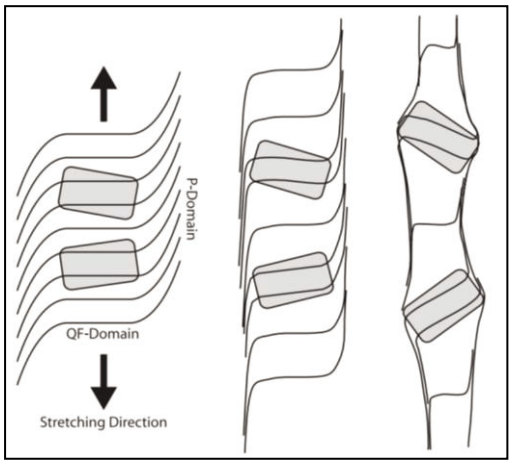

Figure 30 Crenulation cleavage causing re-rotation of porphyroblasts. Time proceeds from left to right, with the porphyroblasts recording the foliation within. Figure from (Johnson et al. 2006)

Looking at the cross-section, the angle of the contact is between the dome and the greenstone belt is 60-80^{o}, indicating a preference for normal movement.

4. CONCLUSIONS AND FURTHER WORK

Bringing the evidence from all three study areas together, I propose the following history for the Yalgoo Dome:

- The Archean greenstone belt was laid down through volcanism and sedimentation.
- D1: At 2960 ± 10 Ma, a tonalite intrusion intruded the greenstones, forming the S_1 metamorphic foliation. Multiple small domes form (less than a few hundred metres long). Foley (1997) suggested these smaller domes were emplaced progressively. Melting and migmatisation occurred, melting both the tonalite and the amphibolite. Leucosomes and felsic melt bands (respectively) form sub-parallel to the S_1 foliation. Various pegmatite dykes intrude through the area at around this time.
- D2: F_2 isoclinal and sheath folds occur, folding the S_1 foliation. It is most likely this event involved a component of N-S shortening due to typical E-W trending F_2 folds. S_2 is parallel to S_1.
- D3: N-S trending upright F_3 open folds occur, resulting from E-W shortening, forming the S_3 foliation. This event overprints the previous foliations. This phase is associated with melting found in axial planar foliations and fold hinges.
- D4: At 2752 ± 13 Ma (with uncertainty as to if the age is representative of the majority of the granite intrusions), various granitic intrusions occur, intruding into the same area, and melting of older rock types at the exposed level had stopped in Study Area 1. These granitic intrusions eroded and entrained xenoliths of the central tonalite. These granitic intrusions may be

linked to the 150^{o} trending porphyritic granite dykes in Study Area 1. Pegmatite dykes, oriented approximately E-W intruded the entire region around this time. These granitic intrusions increased the size of the dome to be what it is today; approximately 95 kilometres long and 50 kilometres wide.

- D2+: A late crenulation cleavage occurred, and is recorded only in the weakest units of the greenstones on the boundary of the dome. We cannot determine the relative age of this event due to lack of overprinting relationships, except to say it was post-D2. It is most likely a local and minor event. This crenulation cleavage caused re-rotation of porphyroblasts and added further complexities to the area.

The detailed mapping of a small dome in Study Area 1, along with evidence of sheath folds developed in D_2, argues against the superposed fold model proposed by Myers and Watkins (1985). This work has examines the evidence, and supports of the work by Foley (1997) and Rey *et al.* (1999). The granitoids of the Yalgoo Dome were emplaced through smaller domes, progressively intruding in single events recorded by sheath folds and domes developed at the scale of hundreds of metres. The normal movement recorded at the contact zone of the large Yalgoo Dome also supports this hypothesis

There is still much work to do on the Yalgoo Dome to determine it's complicated history in more detail:

- Investigate the extent of the migmatitic core, and its geometry.
- Determine if the dextral shearing in Study Area 1, is dextral all across the region, of if in fact it turns to sinistral shearing in the west as we would expect on the other limb of a large F_3 fold.

- P-T-t paths of the schists at the margins of the dome.
- Investigate if there is any intrusive dykes in the greenstones beyond the dome, so as to determine the extent of the granitoid intrusions.
- Investigate the kinematics of the domes margin more closely, to see if the strike-slip component suggested by Rey *et al.* (1999) exists and what effect it has on the formation history.
- Investigate the nature of the dome-greenstone boundary in more detail, looking at the 3D geometries of the dykes and xenoliths.

REFERENCES

FOLEY B. J. 1997. Reassessment of the Archean tectonics in the Murchison Province, Western Australia. *Abstracts - Geological Society of Australia* 46, 23.

GEE R. D. 1979. Structure and tectonic style of the Western Australian Shield. *Tectonophysics* 58, 327-369.

GEE R. D., BAXTER J. L., WILDE S. A. & WILLIAMS I. R. 1981. Crustal development in the Archaean Yilgarn Block, Western Australia. *Special Publication - Geological Society of Australia*, 43-56.

JOHNSON S. E., DUPEE M. E. & GUIDOTTI C. V. 2006. Porphyroblast rotation during crenulation cleavage development; an example from the aureole of the Mooselookmeguntic Pluton, Maine, USA. *Journal of Metamorphic Geology* 24, 55-73.

MACGREGOR A. M. 1951. Some milestones in the Precambrian of Southern Rhodesia [presidential address]. *Proceedings of the Geological Society of South Africa*.

MUHLING P. C. & LOW G. H. 1977. Yalgoo, Western Australia. *1:250 000 Explanatory Notes*.

MYERS J. S. & WATKINS K. P. 1985. Origin of granite- greenstone patterns, Yilgarn Block, Western Australia. *Geology* 13, 778-780.

PATERSON S. R., VERNON R. H. & TOBISCH O. T. 1989. A review of criteria for the identification of magmatic and tectonic foliations in granitoids. *Journal of Structural Geology* 11, 349-363.

REY P., COSTA S., VANDERHAEGHE O. & FOLEY B. 1999. Archaean regional strain field in the Yilgarn Craton (WA); fold superposition or incremental strain field interferences? *Abstracts - Geological Society of Australia* 53, 221-222.

TARNEY J. & WINDLEY B. F. 1981. Marginal basins through geological time. *Philosophical Transactions of the Royal Society of London, Series A: Mathematical and Physical Sciences* 301, 217-232.

VAN KRANENDONK M. J. 2010. Two types of Archean continental crust: plume and plate tectonics on early earth. *American Journal of Science* 310, 1187-1209.

VAN KRANENDONK M. J., IVANIC T. J., WINGATE M. T. D., KIRKLAND C. L. & WYCHE S. 2013. Long-lived, autochthonous development of the archean murchison domain, and implications for yilgarn craton tectonics. *Precambrian Research* 229, 49-92.

WATKINS K. P. & HICKMAN A. H. 1990. Excursion no. 2: Murchison granite-greenstone terrain. Part 1: Geology of the Murchison Province granite-greenstone terraine, Western Australia. Paper presented at Third international Archaean symposium, Perth, 1990, excursion guidebook(unpubl.).

WEINBERG R. F. & MARK G. 2008. Magma migration, folding, and disaggregation of migmatites in the Karakoram shear zone, Ladakh, NW India. *Geological Society of America Bulletin* 120, 994-1009.

WEINBERG R. F., VAN DER BORGH P., BATEMAN R. J. & GROVES D. I. 2005. Kinematic history of the Boulder-Lefroy shear zone system and controls on associated gold mineralization, Yilgarn Craton, Western Australia. *Economic Geology and the Bulletin of the Society of Economic Geologists* 100, 1407-1426.

WINDLEY B. F. 1993. Uniformitarianism today: plate tectonics is the key to the past. *Journal - Geological Society (London)* 150, 7-19.

YIN A. 2004. Gneiss domes and gneiss dome systems. *Special Paper - Geological Society of America* 380, 1-14.

ZEGERS T. E., WIJBRANS J. R. & WHITE S. H. 1999. 40Ar/39Ar age constraints on tectonothermal events in the Shaw area of the eastern Pilbara granite–greenstone terrain (W Australia): 700 Ma of Archean tectonic evolution. *Tectonophysics* 311, 45-81.

ZIBRA I. 2012. Syndeformational granite crystallisation along the Mount Magnet greenstone belt, Yilgarn Craton; evidence of large-scale magma-driven strain localisation during Neoarchean time. *Australian Journal of Earth Sciences* 59, 793-806.

APPENDIX A

A review of Archean tectonics and how this is expressed in terms of metamorphism and structures

Word Count: 3144

Introduction

The Archean is the second geological eon, extending from 3.8-2.5 Ga. There are several structural and petrological characteristic features of the Archean that do not have modern analogues and are unique to that time period. Archean regions contain two types of terranes: low-grade, volcanic-dominated greenstone-granite terranes in the upper crust, high-grade granulites and gneisses in the mid-lower crust (Tarney & Windley 1981; Windley 1993). The key features of Archean terranes are greenstone belts, diapirs and granite domes, and komatiites. Understanding what these features represent is the key to understanding the global processes active in the Archean.

There is much debate as to whether or not Phanerozoic style plate tectonics occurred in the Archean, to what extent and form it operated under, and to what other processes where also active. This review aims to look at the characteristic features of the Archean, what they may mean, and the various schools of thought for global processes in the Archean.

It is important to consider this topic as it provides insights into how the Earth became to be what we see today. Extensive work has been done on Phanerozoic processes and features, but that all came from somewhere. That somewhere is the Archean, which makes this topic incredibly relevant.

Characteristic Features of the Archean

Greenstone belts

Greenstone belts are generally composed of mafic to felsic lavas and pyroclastics, along with sedimentary successions such as conglomerates, greywackes, sandstones, quartzites and shales. These rocks are metamorphosed to greenschist facies, with low-moderate deformation (Tarney & Windley 1981). Greenstone belts are generally found only in the Archean, although some are found in the Proterozoic. Archean greenstone belts are dominated by synclinal structures, which are thought to be formed through compression caused by diapiric batholith intrusions (Hamilton 1998). Similar thick sedimentary successions can be found in the Phanerozoic, but the key volcanics found in the Archean, such as komatiites, are not as common (Tarney & Windley 1981). The largest difficulty with greenstone belts, is that the interpretations in the literature depends on the author's opinion of whether or not plate tectonics was active during the Archean. If you can be certain one way, then interpreting greenstone belts becomes easier. As we currently cannot conclusively say what the global process was in the Archean, the meaning of greenstone belts is unclear. Tarney and Windley (1981) argue that greenstone belts are analogues of modern marginal basins, where Hamilton (1998, 2011) is adamant that greenstone belts have no modern analogue and are formed by a different regime. Other researchers suggest that greenstone belts represent laterally continuous volcanic sedimentary sequences, interpreting them to be ancient magmatic arcs. This interpretation comes from the idea that the Archean was dominated by mantle plumes. Still other researchers argue that plate tectonics was active, and so greenstone belts are an amalgamation of oceanic crust, island arcs and accretionary prisms. Collins and van Kranendonk (1998) suggest that greenstone belts are analogous to continental flood basalts.

Granite domes and diapirs

There are two main styles of granite doming in Archean successions; diapric and tectonic doming. However, granitoids preferentially intrude into existing granitoids, resulting in cored domes, and hence the Archean granites are generally more deformed than the surrounding greenstones (Zegers *et al.* 1999). Diapiric domes are not related to tectonics, and are mushroom shaped intrusions that rise because they become either thermally buoyant or compositionally buoyant. The compositional buoyancy requires either the sequences being deposited on top to be more dense than the assemblages below (density inversion), or for the assemblages below to change and become less dense that the overlying rocks. After 3.6 Ga, the Archean felsic crust had cooled sufficiently to permit mafic-ultramafic magmas to rise and erupt. When these magmas and/or lavas crystallised, they became more dense and so sank into the crust, forming diapiric batholiths (Hamilton 2011). The Mount Edgar Batholith in the Pilbara Craton of Western Australia is considered to have formed through the density inversion of a thick greenstone sequence (Collins & van Kranendonk 1998). Diapir emplacement is independent of tectonic processes, and can occur due to either solid-state or magmatic processes.

Tectonic domes however, are formed through tectonic stresses, in either compressional or extensional regimes. In a compressional regime, granites rise through thermal buoyancy and can influence the position of antiforms in the rock packages it intruded into (Weinberg *et al.* 2003). In an extensional regime, granites can rise due to decompression and form structures not too dissimilar from metamorphic core complexes. The key difference between these granite domes and metamorphic core complexes is the normal faulting around the domes. In metamorphic core complexes, there is normal faulting on two sides of the intrusion, where these Archean granites have normal faults extending radially (for

example, the Raeside Batholith). It is suggested that these granites were emplaced under generalised horizontal stretching (Weinberg & van der Borgh 2008).

Granite domes are very useful in terms of constraining structural events in the Archean, in particular in cratons such as the Yilgarn, where granitic bodies are thought to be fundamental in its development. Granites in the Archean can exist as pre-, syn- or post-tectonic intrusions (Zegers *et al.* 1999), and using granites as geochronological constraints has been described extensively by Weinberg *et al.* (2003).

Many Archean granite domes can be related to contemporaneous felsic volcanism (Kroner & Layer 1992). However, much discussion is still occurring on what caused the emplacement of these granites, which relates to the different schools of thought on Archean tectonics.

Komatiites

Komatiites are ultra-mafic lavas that are rich in magnesium and were erupted at very high temperatures with a low viscosity (Thompson Stiegler *et al.* 2012). It is thought that they are the result of large amounts of partial melting, within deep mantle plumes. The excess heat from the plumes and the pressure at great depth, allows for komatiitic melts rather than basaltic melts to form (Herzberg 1992). Nesbitt *et al.* (1979) and Herzberg (1992) suggested that komatiites had to form deep within the earth, at depths of about 400 km. However, Sleep and Windley (1982) found that if the earth has been cooling since the Archean and was hotter than present mantle temperatures, then komatiites could have been derived from shallower depths of <70 km. Komatiites are voluminous, and due to their intense heat are thought to be a mechanism of high heat loss in the Archean (Hamilton 1998). Most komatiites are found in Archean greenstone belts, with younger komatiites being rare (Parman *et al.* 1997).

There are a few interpretations of what komatiites represent. Chavagnac (2004) interpreted them to have erupted at a mid-ocean ridge forming an oceanic plateau. Parman *et al.* (1997) found that the 3.5 Ga komatiites from the Barberton Greenstone Belt in South Africa, were hydrous, and a uniformitarian view would suggest that they formed in a subduction setting. If subduction was the case, then Archean subduction zones would be 100-200^{o}C hotter than Phanerozoic subduction zones. Although komatiites are rarely found in the Phanerozoic, which means they are not directly related to subduction zones, therefore this interpretation doesn't hold much water. Therefore Parman *et al.* (1997) suggested that the early Earth accretion left high abundances of volatiles in the mantle. Therefore, komatiites could represent a degassing period, which shows that the mantle was wetter than Phanerozoic mantle, but less than 100^{o}C hotter.

Archean global processes

The key question about the Archean is what global process was dominant at the time. Was it Phanerozoic style plate tectonics? Was it a modified or evolving style of plate tectonics? Or was it something completely different? These are the three main schools of thought on the matter.

Applying the principle of uniformitarianism

The principle of uniformitarianism states that the processes we see occurring now are the same as what has occurred in the past. Therefore, Phanerozoic style plate tectonics must have occurred in the Archean. Windley (1993) proposed that despite the hotter conditions of the Archean, tectonic and geochemical processes are fundamentally the same in the Archean as what we see today. He argues that the principle of uniformitarianism implies that the theory of plate tectonics can help us understand the Archean, but it does not mean

that it is identical to the Phanerozoic. Many Archean features occur as a result of the greater heat production, which is thought to be three times higher than that of the present. If this is the case, then the mantle would be hotter, the depth of melting would have been deeper, the continental lithosphere and oceanic crust would have been thicker, and the spreading rates of mid-ocean ridges would have been 2-3 times faster than today's rates (Sleep & Windley 1982). Sleep and Windley (1982) suggested a hypothesis that the Archean mantle was hot, and that Archean oceanic crust had a thickness of at least 20 km. This thick oceanic crust is supported by evidence from the Abitibi greenstone belt (Goodwin 1976; Windley & Davies 1978), West Greenland (Wells 1979), and the Fiskenaesset anorthosite complex (Myers & Platt 1977). A consequence of considerably thicker Archean oceanic crust, is that at spreading ridges the magma chamber and associated gabbro complex would also be much larger. Although, the thickness of the pillow basalt and sheeted dyke complexes would not change as they are influenced by the conduction of heat laterally, which is dependent on spreading rate (Cann 1974).

Due to the higher temperature, the asthenosphere would have had a lower viscosity, and so plates could move around easier and be subducted rapidly. This is supported by models of thick buoyant plates over a hot mantle, which show that the resistance to plate motion would have been much lower in the Archean (Nisbet & Fowler 1983). If the plates were being subducted at a much younger age, they would have been more buoyant and so pose a problem for subduction. Also, the idea of thick oceanic crust does not match with the findings of Taira *et al.* (1992) or Davies (2006), who both suggest that the Archean would have thin crust. However Burke *et al.* (1976) show that subduction of buoyant material was occurring in the Archean more frequently than in the Phanerozoic, and both the buoyancy and thickness problems can be overcome by delamination of the upper crust (Hoffman & Ranalli 1988). Further to this, Zegers *et al.* (2001) found that between 3480-3420 Ma,

extension in the upper and middle crust occurred simultaneously and had associated TTG granitoid intrusions, along with felsic and ultramafic-mafic volcanics. These two events, the extension and intrusion doesn't fit with either Phanerozoic subduction or mantle plume dominated settings. However, it does match with models suggesting lithosphere delamination.

Although, delamination models were discounted by Van Kranendonk (2011) as delamination should continue to occur beyond the Archean, if Archean continents were as thick as those in the Phanerozoic.

Shirey and Richardson (2011) conducted a study on diamonds from deep in the cratonic keel. They found that eclogitic diamonds were present back to 3.0 Ga. As eclogite can only be formed in shallow crust (>100 km), and the eclogitic diamonds were formed at depths of 125-175 km, the conclusion must be made that the eclogite were transported downwards. The only processes of doing this is via subduction or through delamination of the oceanic crust. If (Van Kranendonk 2011) is correct, then subduction must be active in the Archean.

de Ronde and de Wit (1994) interpreted the Barberton Greenstone Belt using Phanerozoic processes, and suggested that mid-ocean ridges, magmatic arcs, trenches, subduction and accretion all played a role in its formation. This is disputed widely, and other researchers suggest that an Archean-unique process formed this greenstone belt.

An unique Archean global process

The second school of thought is that another process, unique to the Archean and represented by granite-greenstone terranes, was in operation through the Archean. Phanerozoic style plate tectonics only developed in the Proterozoic, when the other process(es) went extinct.

Hamilton (1998, 2011)argues that Phanerozoic style plate tectonics could not have been active during the Archean, as characteristic convergent margin assemblages and structures (such as blueschists or evidence of deep continental crust subduction) are not seen in the Archean or have an Archean analogue. These characteristic features have not been found before the Neoproterozoic, implying that Phanerozoic style plate tectonics could not have operated before then. He further argues that the granite-greenstone terranes and voluminous ultra-mafic lavas represent heat loss in the Archean, by voluminous magmatism from a much hotter mantle, and that greenstone belts were formed by compression from diapiric batholiths. These are all characteristic features of the Archean and have no modern analogues, therefore Phanerozoic style plate tectonics cannot have been present in the Archean.

Barley *et al.* (2005) found that in the Late Archean and into the Early Paleoproterozoic, the global tectonic regime was changing from a plume driven regime to a quieter period little active processes. They argue that the Great Oxygenation Event around 2.4 Ga represents changing geologic regimes as the sinks for oxygen, rather than the source, may have changed. The relationship between tectonics in the Phanerozoic and environmental change has been extensively studied, where periods of super-plume events have associated higher sea levels and greenhouse conditions, follwed by lower sea levels and glaciations. It is suggested that the glaciation and oxidation of the continental crust after 2.4 Ga represents a Phanerozoic-style plate tectonic regime beginning, however before that a different global process was active.

Choukroune *et al.* (1995) states that the granite-greenstones are never found in Phanerozoic orogenic belts, which differ from Archean orogens because they generally have a consistent structural trend. They propose that the Archean cratons were not rigid

during their formation, and that continental crust was either created or reworked by episodic mantle plume activity.

Davies (1995) proposed a model where stratification of the mantle became unstable over a few hundred Ma in the early earth and resulted in mantle overturning. This is where the cooler upper mantle is replaced by hotter material from the lower mantle, causing "global convulsions." However, he also argues that these models would allow plate tectonics to occur between the convulsions but was reset every few hundred Ma.

Van Kranendonk *et al.* (2004) also proposed a model of mantle overturn, resulting from partial melting of the mid-crust. However, at one point the mantle did not completely overturn due to the crystallisation of the rising granitoids, leaving a gravitational instability that could be reactivated over time, forming the granite-greenstone terranes.

Hamilton (1998) suggests that rifting and convergence of plates was active around 2.0 Ga, and reach Phanerozoic style around 0.8 Ga. There was a transition from the regime represented by granite-greenstone assemblages, to plate tectonics from about 2.6-2.0 Ga. He suggests that the change may be brought about due to dense, hydrated Archean crust sinking into the mantle, increasing its water and carbon dioxide content.

An evolving plate tectonics

The third school of thought is that Phanerozoic style plate tectonics was in a development stage in the Archean, or was modified in some form due to the differences in crust and mantle properties. Dewey and Windley (1981) state that while the principle of uniformitarianism cannot be applied precisely to the Archean, but some form of plate tectonic process was active in the Archean, and global processes evolved rather than changed type in the Archean.

The two main types of Archean tectonic belts, granulite-gneiss and greenstone belts, are both unique to the Archean, however they did continue to form to a lesser extent into the Proterozoic (Tarney & Windley 1981). Sleep and Windley (1982) suggest that this is evidence, along with Proterozoic ophiolites, for a development of the Wilson Cycle.

Sizova *et al.* (in press) proposes two forms of collision that differ from Phanerozoic collision, if the Archean upper mantle temperature was at least 80-100 K above modern temperatures. These two collisional models, the 'truncated hot collision regime' and the 'two-sided hot collision regime,' both involve the break off of shallow slabs, preventing the formation of ultra-high pressure metamorphic rocks. This change in style from these hot collisional regimes to Phanerozoic collisional regimes in the Neoproterozoic as the Earth cooled, explains why ultra-high pressure metamorphic rocks (representing deep continental crust subduction) are not seen in the geologic record until the Neoproterozoic, thus allowing plate tectonics to occur before then.

Hickman (2004) suggests that before 2900 Ma Archean terranes have dome and basin patterns, where after 2900 Ma they exhibit linear structures. The Pilbara craton is characterised by dome and basin patterns, but the Yilgarn craton is characterised by NNE-SSW shear zones. Davies (1998) suggests that these different characterisation patterns are due to the evolution of tectonic processes.

Coltice *et al.* (2009) argue that continental crust growth is an episodic process. There are major crustal growth events related to mantle magmatism and orogenesis at 2700, 2500, 1900, 1100, 480, 280 and 100 Ma. Evidence for continental crust dating back to 4.1 Ga also exists by way of zircons. Aspler and Chiarenzelli (1998) suggest that Archean supercontinents existed between 2750 and 2650 Ma during a time of crustal growth. In their review of Archean tectonics, Van Kranendonk *et al.* (2007) suggest that as the

Archean was hotter, the plates were less stable and so were not as large as Phanerozoic plates. Therefore there could not have been large scale plate tectonics. Rather, plate tectonics developed as the plates themselves developed. Sleep and Windley (1982) also suggest that ever since continental crust was formed, there would be collisions and some form of subduction, just not to the same extent as seen in the Phanerozoic.

Discussion

The difficulties of analysing Archean tectonics and determining Archean processes, are that much of the evidence is ambiguous, and can have multiple interpretations. There are many characteristic features seen in the Archean that appear to be unique, and so may well have been formed by unique processes. However, it is also possible that these processes were early forms of Phanerozoic processes (plate tectonics), and were simply expressed differently due to the Earth itself being an early form of Phanerozoic Earth. I suggest that it does not matter if diagnostic features of Phanerozoic style tectonics are not found in the Archean, because I would not expect it to. They Archean was very different to the Phanerozoic, yet plate tectonics is a fundamental process of the Earth, and has developed with the Earth from the beginning.

Conclusion

Much discussion of Archean tectonics and how to interpret Archean terranes has occurred for many years with still no conclusive answers. There are two key Archean terranes, granulite-gneiss and greenstone-granite terranes and they are dominated by komatiites, greenstones, granite domes and diapirs. These features can be interpreted in different ways in terms of processes of formation. The main schools of thought are that they were formed through Phanerozoic style plate tectonics, a process unique to the Archean, or through a developing or modified plate tectonics.

References

ASPLER L. B. & CHIARENZELLI J. R. 1998. Two Neoarchean supercontinents? Evidence from the Paleoproterozoic. *Sedimentary Geology* **120**, 75-104.

AYRES L. D. 1983. Bimodal volcanism in Archean greenstone belts exemplified by greywacke composition, Lake Superior Park, Ontario. *Canadian Journal of Earth Sciences* **20**, 1168-1194.

BARLEY M. E., BEKKER A. & KRAPEZ B. 2005. Late Archean to Early Paleoproterozoic global tectonics, environmental change and the rise of atmospheric oxygen. *Earth and Planetary Science Letters* **238**, 156-171.

BURKE K., DEWEY J. F. & KIDD W. S. F. 1976. Dominance of horizontal movements, arc and microcontinental collisions during the later permobile regime. Paper presented at The early history of the Earth(unpubl.).

CANN J. R. 1974. A model for oceanic crustal structure developed. *Geophysical Journal of the Royal Astronomical Society* **39**, 169-187.

CHAVAGNAC V. 2004. A geochemical and Nd isotopic study of Barberton komatiites (South Africa): Implication for the Archean mantle. *Lithos* **75**, 253-281.

CHOUKROUNE P., BOUHALLIER H. & ARNDT N. T. 1995. Soft lithosphere during periods of Archaean crustal growth or crustal reworking. *Geological Society Special Publications* **95**, 67-86.

COLLINS W. J. & VAN KRANENDONK M. J. 1998. Partial convective overturn of Archaean crust in the East Pilbara Craton, Western Australia; driving mechanisms and tectonic implications. *Journal of Structural Geology* **20**, 1405-1424.

COLTICE N., BERTRAND H., REY P., JOURDAN F., PHILLIPS B. R. & RICARD Y. 2009. Global warming of the mantle beneath continents back to the Archaean. *Gondwana Research* **15**, 254-266.

DAVIES G. F. 1995. Punctuated tectonic evolution of the Earth. *Earth and Planetary Science Letters* **136**, 363-379.

DAVIES G. F. 1998. Plates, plumes, mantle convection, and mantle evolution. Paper presented at The Earth's mantle; composition, structure, and evolution(unpubl.).

DAVIES G. F. 2006. Gravitational depletion of the early Earth's upper mantle and the viability of early plate tectonics. *Earth and Planetary Science Letters* **243**, 376-382.

DE RONDE C. E. J. & DE WIT M. J. 1994. Tectonic history of the Barberton greenstone belt, South Africa: 490 million years of Archean crustal evolution. *Tectonics* **13**, 983-1005.

DEWEY J. F. & WINDLEY B. F. 1981. Growth and differentiation of the continental crust. *Philosophical Transactions of the Royal Society of London, Series A: Mathematical and Physical Sciences* **301**, 189-206.

DIMROTH E., IMREH L., COUSINEAU P., LEDUC M. & SANSCHAGRIN Y. 1985. Paleogeographic analysis of mafic submarine flows and its use in the exploration for massive sulphide deposits. *Special Paper - Geological Association of Canada* **28**, 203-222.

DIMROTH E., IMREH L., ROCHELEAU M. & GOULET N. 1982. Evolution of the south-central part of the Archean Abitibi Belt, Quebec; Part I, Stratigraphy and paleogeographic model. *Canadian Journal of Earth Sciences = Journal Canadien des Sciences de la Terre* **19**, 1729-1758.

FISHER R. V. 1982. Debris flows and lahars. *Short Course Notes - Geological Association of Canada* **2**, 136-220.

FOLEY B. J. 1997. Reassessment of the Archean tectonics in the Murchison Province, Western Australia.

Abstracts - Geological Society of Australia **46**, 23.

FRASER G., MCAVANEY S., NEUMANN N., SZPUNAR M. & REID A. 2010. Discovery of early Mesoarchean crust in the eastern Gawler Craton, South Australia. *Precambrian Research* **179**, 1-21.

GEE R. D. 1979. Structure and tectonic style of the Western Australian Shield. *Tectonophysics* **58**, 327-369.

GEE R. D., BAXTER J. L., WILDE S. A. & WILLIAMS I. R. 1981. Crustal development in the Archaean Yilgarn Block, Western Australia. *Special Publication - Geological Society of Australia*, 43-56.

GOODWIN A. M. 1976. Archean volcanoes in southwestern Abitibi Belt, Canada; form, composition and development. *Abstracts with Programs - Geological Society of America* **8**, 888.

HAMILTON W. B. 1998. Archean magmatism and deformation were not products of plate tectonics. *Precambrian Research* **91**, 143-179.

HAMILTON W. B. 2011. Plate tectonics began in Neoproterozoic time, and plumes from deep mantle have never operated. *Lithos* **123**, 1-20.

HERZBERG C. 1992. Depth and degree of melting of komatiites. *Journal of Geophysical Research: Solid Earth* **97**, 4521-4540.

HICKMAN A. H. 2004. Two contrasting granite-greenstone terranes in the Pilbara Craton, Australia; evidence for vertical and horizontal tectonic regimes prior to 2900 Ma. *Precambrian Research* **131**, 153-172.

HOFFMAN P. F. & RANALLI G. 1988. Archean oceanic flake tectonics. *Geophysical Research Letters* **15**, 1077-1080.

JOHNSON S. E., DUPEE M. E. & GUIDOTTI C. V. 2006. Porphyroblast rotation during crenulation cleavage development; an example from the aureole of the Mooselookmeguntic Pluton, Maine, USA. *Journal of Metamorphic Geology* **24**, 55-73.

KRONER A. & LAYER P. W. 1992. Crust formation and plate motion in the early Archean. *Science* **256**, 1405-1411.

MACGREGOR A. M. 1951. Some milestones in the Precambrian of Southern Rhodesia [presidential address]. *Proceedings of the Geological Society of South Africa*.

MUHLING P. C. & LOW G. H. 1977. Yalgoo, Western Australia. *1:250 000 Explanatory Notes*.

MYERS J. S. & PLATT R. G. 1977. Mineral chemistry of layered Archaean anorthosite at Majorqap qava, near Fiskenaesset, Southwest Greenland. *Lithos* **10**, 59-72.

MYERS J. S. & WATKINS K. P. 1985. Origin of granite- greenstone patterns, Yilgarn Block, Western Australia. *Geology* **13**, 778-780.

NESBITT R. W., SUN S. S. & PURVIS A. C. 1979. Komatiites; geochemistry and genesis. *The Canadian Mineralogist* **17, Part 2**, 165-186.

NISBET E. G. & FOWLER C. M. R. 1983. Model for Archean plate tectonics. *Geology* **11**, 376-379.

PARMAN S. W., DANN J. C., GROVE T. L. & DE WIT M. J. 1997. Emplacement conditions of komatiite magmas from the 3.49 Ga Komati Formation, Barberton Greenstone Belt, South Africa. *Earth and Planetary Science Letters* **150**, 303-323.

PATERSON S. R., VERNON R. H. & TOBISCH O. T. 1989. A review of criteria for the identification of magmatic and tectonic foliations in granitoids. *Journal of Structural Geology* **11**, 349-363.

PIDGEON R. T. & HALLBERG J. A. 2000. Age relationships in supracrustal sequences of the northern part of the Murchison Terrane, Archaean Yilgarn Craton, Western Australia; a combined field and zircon U-Pb study. *Australian Journal of Earth Sciences* **47**, 153-165.

REY P., COSTA S., VANDERHAEGHE O. & FOLEY B. 1999. Archaean regional strain field in the Yilgarn Craton (WA); fold superposition or incremental strain field interferences? *Abstracts* -

Geological Society of Australia **53**, 221-222.

SHIREY S. B. & RICHARDSON S. H. 2011. Start of the Wilson Cycle at 3 Ga Shown by Diamonds from Subcontinental Mantle. *Science* **333**, 434-436.

SIZOVA E., GERYA T. & BROWN M. in press. Contrasting styles of Phanerozoic and Precambrian continental collision. *Gondwana Research*.

SLEEP N. H. & WINDLEY B. F. 1982. Archean plate tectonics: constraints and inferences. *Journal of Geology* **90**, 363-379.

TAIRA A., PICKERING K. T., WINDLEY B. F. & SOH W. 1992. Accretion of Japanese island arcs and implications for the origin of Archean greenstone belts. *Tectonics* **11**, 1224-1244.

TARNEY J. & WINDLEY B. F. 1981. Marginal basins through geological time. *Philosophical Transactions of the Royal Society of London, Series A: Mathematical and Physical Sciences* **301**, 217-232.

THOMPSON STIEGLER M., COOPER M., BYERLY G. R. & LOWE D. R. 2012. Geochemistry and petrology of komatiites of the Pioneer Ultramafic Complex of the 3.3 Ga Weltevreden Formation, Barberton greenstone belt, South Africa. *Precambrian Research* **212–213**, 1-12.

VAN KRANENDONK M. J. 2010. Two types of Archean continental crust: plume and plate tectonics on early earth. *American Journal of Science* **310**, 1187-1209.

VAN KRANENDONK M. J. 2011. Onset of Plate Tectonics. *Science* **333**, 413-414.

VAN KRANENDONK M. J., COLLINS W. J., HICKMAN A. & PAWLEY M. J. 2004. Critical tests of vertical vs. horizontal tectonic models for the Archaean East Pilbara Granite–Greenstone Terrane, Pilbara Craton, Western Australia. *Precambrian Research* **131**, 173-211.

VAN KRANENDONK M. J., HUGH SMITHIES R., HICKMAN A. H. & CHAMPION D. C. 2007. Review: secular tectonic evolution of Archean continental crust: interplay between horizontal and vertical processes in the formation of the Pilbara Craton, Australia. *Terra Nova* **19**, 1-38.

VAN KRANENDONK M. J., IVANIC T. J., WINGATE M. T. D., KIRKLAND C. L. & WYCHE S. 2013. Long-lived, autochthonous development of the archean murchison domain, and implications for yilgarn craton tectonics. *Precambrian Research* **229**, 49-92.

WATKINS K. P. & HICKMAN A. H. 1990. Excursion no. 2: Murchison granite-greenstone terrain. Part 1: Geology of the Murchison Province granite-greenstone terraine, Western Australia. Paper presented at Third international Archaean symposium, Perth, 1990, excursion guidebook(unpubl.).

WEINBERG R. 2005. Kinematic history of the Boulder-Lefroy shear zone system and controls on associated gold mineralization, Yilgarn craton, Western Australia. *Economic Geology and the Bulletin of the Society of Economic Geologists* **100**, 1407-1426.

WEINBERG R. F. & MARK G. 2008. Magma migration, folding, and disaggregation of migmatites in the Karakoram shear zone, Ladakh, NW India. *Geological Society of America Bulletin* **120**, 994-1009.

WEINBERG R. F., MORESI L. & VAN DER BORGH P. 2003. Timing of deformation in the Norseman-Wiluna Belt, Yilgarn Craton, Western Australia. *Precambrian Research* **120**, 219-239.

WEINBERG R. F. & VAN DER BORGH P. 2008. Extension and gold mineralization in the Archean Kalgoorlie Terrane, Yilgarn Craton. *Precambrian Research* **161**, 77-88.

WEINBERG R. F., VAN DER BORGH P., BATEMAN R. J. & GROVES D. I. 2005. Kinematic history of the Boulder-Lefroy shear zone system and controls on associated gold mineralization, Yilgarn Craton, Western Australia. *Economic Geology and the Bulletin of the Society of Economic Geologists* **100**, 1407-1426.

WELLS P. R. A. 1979. Chemical and thermal evolution of Archaean sialic crust, southern West Greenland. *Journal of Petrology* **20**, 187-226.

WINDLEY B. F. 1993. Uniformitarianism today: plate tectonics is the key to the past. *Journal - Geological Society (London)* **150**, 7-19.

WINDLEY B. F. & DAVIES F. B. 1978. Volcano spacings and lithospheric/crustal thickness in the Archaean. *Earth and Planetary Science Letters* **38**, 291-297.

YIN A. 2004. Gneiss domes and gneiss dome systems. *Special Paper - Geological Society of America* **380**, 1-14.

ZEGERS T. E., NELSON D. R., WIJBRANS J. R. & WHITE S. H. 2001. SHRIMP U-Pb zircon dating of Archean core complex formation and pancratonic strike-slip deformation in the East Pilbara Granite-Greenstone Terrain. *Tectonics* **20**, 883-908.

ZEGERS T. E., WIJBRANS J. R. & WHITE S. H. 1999. 40Ar/39Ar age constraints on tectonothermal events in the Shaw area of the eastern Pilbara granite–greenstone terrain (W Australia): 700 Ma of Archean tectonic evolution. *Tectonophysics* **311**, 45-81.

ZIBRA I. 2012. Syndeformational granite crystallisation along the Mount Magnet greenstone belt, Yilgarn Craton; evidence of large-scale magma-driven strain localisation during Neoarchean time. *Australian Journal of Earth Sciences* **59**, 793-806.

APPENDIX B

Word Count: 2159

A review of the Yalgoo Dome, Yilgarn Craton, Western Australia.

The Yalgoo Dome is a unique structure in terms of Yilgarn geology, and has the potential to further our understanding of granite-greenstone terrane patterns. The current debate is whether Archean granite-greenstone terrane patterns are formed through diapiric emplacement, or through Phanerozoic style plate tectonics, such as dome-and-basin fold interference patterns. The aim of this review is to put the Yalgoo Dome into geologic context, and look through the findings of previous work done on the area. The Yalgoo Dome is located just south of the town of Yalgoo, a small, historic mining town in outback Western Australia, about 600 kilometres north-east of Perth and 200 kilometres east of Geraldton. Geologically speaking, the Yalgoo Dome is in the Murchison Province of the Yilgarn Craton, Western Australia.

The Yilgarn Craton

There are two Archean cratons that make up the West Australian Craton in Western Australia; the smaller Pilbara Craton in the north and the larger Yilgarn Craton in the south (Figure 1). The Yilgarn Craton is composed of three provinces; the Eastern Goldfields Province in the east, the Murchison Province in the west and the Southern Cross Province in the centre(Watkins & Hickman 1990). The Murchison and the Southern Cross Provinces are combined to make the Youanmi Terrane (Van Kranendonk *et al.* 2013). The Yilgarn Craton is an important gold province, with mining operations throughout, although mostly focused in the Eastern Goldfields Province. Figure 2 shows the dominant north-northwest trending

structures in the Yilgarn Craton, and example of this being the Norseman-Wiluna Belt in the Eastern Goldfields Province which extends for hundreds of kilometres (Weinberg *et al.* 2003; Weinberg 2005). The Yilgarn Craton is a granite-greenstone terrane, which is composed dominantly of curved greenstone belts of sedimentary and/or volcanic rocks, and large elliptical regions of granitoid rocks (Gee 1979).

The field area of this work is located within the Murchison Province of the Yilgarn Craton, and is unique in the Yilgarn as it is a dome structure similar to those seen in the Pilbara Craton (Gee 1979). Although the dome is elongate north-south, possibly corresponding to the north-northwest trending structures seen throughout the Yilgarn.

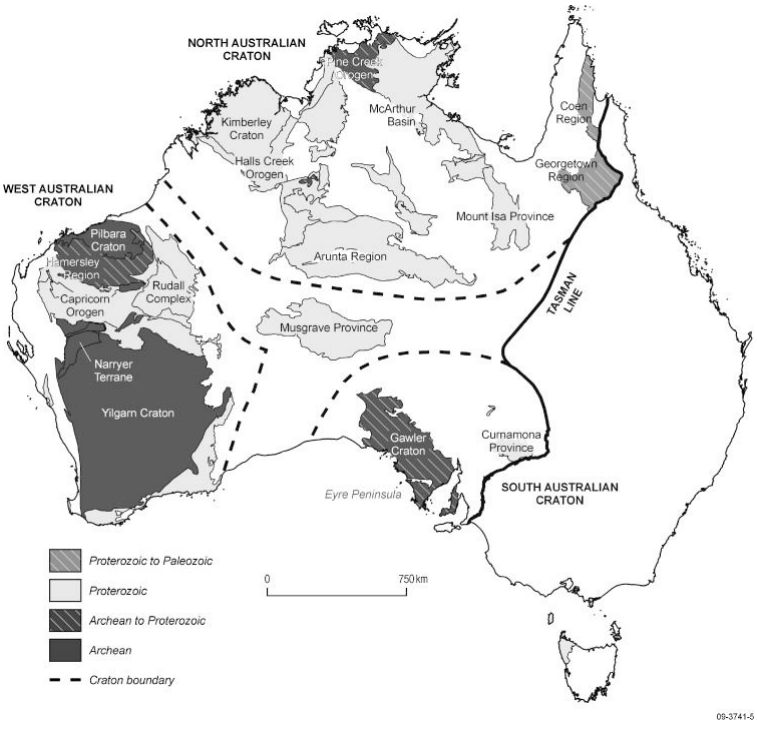

Figure 1 Australian Cratons. Figure from Fraser *et al.* (2010)

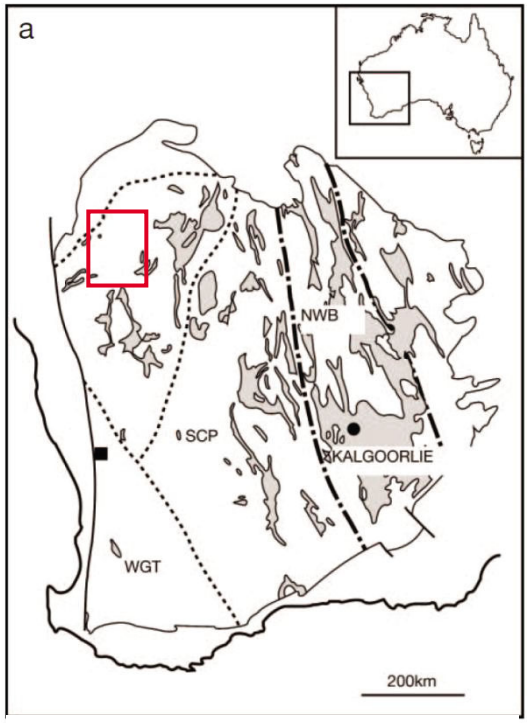

Figure 2 NNW-SSE trending structures in the Yilgarn Craton, the field area of this work highlighted by a red box. Figure from Weinberg *et al.* (2005).

The Murchison Province

The Murchison Province is the western province of the Yilgarn Craton, and makes up part of the Youanmi Terrane. Most of the mining in the province has been around gold production. Since the 1890s, the Murchison province has been a very important gold province, although the mining of other minerals has been almost non-existent. The only major mines of other minerals are the now historic Koolanooka iron-ore mine, and the Cu-Zn mine at Golden Grove, on the eastern margin of the Yalgoo Dome.

Watkins and Hickman (1990) proposed a stratigraphic scheme for the Murchison, which involved six crustal components, four of which are granitoid suites and the other two are greenstone sequences, namely the Luke Creek Group and the Mount Farmer Group. The Luke Creek Group is composed of four volcanic formations, which are laterally extensive and can be seen throughout the Murchison. The Mount Farmer Group is composed of discontinuous formations which are generally restricted to single greenstone belts, and are thought to correspond to volcanic centres. Most of the Mount Farmer Group formations are volcanic, except one which is a large epiclastic sedimentary basin. These two greenstone sequences are combined stratigraphically to make the Murchison Supergroup (Watkins & Hickman 1990).

The four granitoid suites are: pegmatite banded gneiss, recrystallised monzogranite, and post folding granitoids which are divided into two suites based on petrology and geochemistry. These granitoids intruded the Murchison Supergroup in three phases of magmatism, with the post folding granitoids being contemporaneous to each other.

The pegmatite banded gneiss is made up of medium grained, compositionally banded monzogranite and granodiorite, interlayed with pegmatite bands. All banding is on the order of centimetres, none more than ten centimetres thick. The gneiss is found in the recrystallised monzogranite as enclaves and rafts (Myers & Watkins 1985; Watkins & Hickman 1990)

The recrystallised monzogranite now contains only metamorphic textures due to recrystallisation which destroyed the igneous fabric. These monzogranites are located between the greenstone belts and occur in three different textures: equigranular, porphyritic and sparsely porphyritic with less than 5% phenocrysts (Myers & Watkins 1985; Watkins & Hickman 1990).

The post folding granitoids are split into two suites (I and II) based on petrology and geochemistry. Suite I contains tonalite, granodiorite, monzogranite and trondhjemite, where suite II contains quartz rich monzogranite and syenogranite. There is no consistent relationship between these suites and shear zones, as they are offset by most, but cut through others. There are only three circumstances in which these plutons occur: within greenstone belts, in the contact between the recrystallised monzogranite and the greenstone belts, and at the tip of greenstone belts within the monzogranite.

However, Pidgeon and Hallberg (2000) found inconsistences with this stratigraphic scheme, and concluded that a formal scheme for the greenstones of the Murchison could not be constructed. Instead they proposed 5 informal assemblages for the greenstones, which is outlined in Table 1.

Table 1 Informal stratigraphic scheme proposed by Pidgeon and Hallberg (2000)	
Assemblage 1	Restricted to a thin area trending north-northeast from Mt. Magnet, this assemblage contains a mix of thin units of banded iron formation, komatiite, high Mg basalt, dolerite, andesite, and various schists.
Assemblage 2	Widespread through the area, this assemblage consists of banded iron formation units, which are separated by massive mafic rocks.
Assemblage 3	Continuous over most of the northern part of the Murchison, this assemblage contains interlayered high Mg basal, basalt and komatiite, with many black shale and cherty-tuff horizons.
Assemblage 4	Occurring near major fault and shear systems, this assemblage consists of rhyolititic to dacitic volcanic rocks.
Assemblage 5	Present along major regional shear systems, this assemblage contains graphitic clastic sedimentary rocks, and are structurally placed within Assemblage 3 and 4 rocks.

The greenstones of the Murchison Province are composed chiefly of volcanic derived rocks, indicating that volcanism played a key role in the development of the province. There are three styles of extrusive volcanism found in the Murchison; lava plains, shield volcanoes and stratovolcanoes (Watkins & Hickman 1990).

The lava plains are made up of tholeiitic and/or high magnesium basalts, which are regionally extensive and several kilometres thick. The only lava plains are found in the Luke Creek Group (Watkins & Hickman 1990), which possibly corresponds to Assemblage 3 (Pidgeon & Hallberg 2000). The massive lava flows have limited pillow lavas, and so volcanic centres and distal and proxial facies are difficult to determine. Dimroth *et al.* (1982) describe an Archean greenstone belt in Canada that exhibits similar characteristics, and so it is likely that these eruptions occurred under at least two kilometres of water, with the evidence to suggest this being the absence of vesicles, pillow breccia and limited pyroclastics (Ayres 1983; Watkins & Hickman 1990).

The second style, shield volcanism, is seen through multiple kilometre thick basalts, which are not laterally continuous. These basalts contain pillow lavas and hyaloclastites, which means that distal and proximal facies are discernable

(Watkins & Hickman 1990). These volcanoes may have occurred under a few hundred metres of water, with the evidence to suggest this being the presence of hyaloclastites and limited pyroclastics (Dimroth *et al.* 1985).

The third style, stratovolcanoes, are not well preserved due to erosion, and often the only remains are sedimentary rocks derived from the volcano. However, some of these volcanic piles are a few kilometres thick and several kilometres wide. These volcanoes most likely occurred in shallow water or on land, with the evidence to suggest this being waterlain tuff with depositional structures and lahar deposits (Fisher 1982).

The Murchison Province was deformed and developed by several events. Watkins and Hickman (1990) describe the geological history of the Murchison Province through the Archean in 10 stages:

Stage 1: The Luke Creek Group greenstones are deposited on what is thought to be the basement at about 3000 Ma.

Stage 2: Monzogranite and granodiorite intrude as sheets at about 2900 Ma.

Stage 3: Deformation phase 1; horizontal tectonics cause recumbent folding and thrusting. The pegmatite-banded gneiss was developed through deforming the granitoid intrusions (Stages 2 and 3 could be contemporaneous).

Stage 4: The Mount Farmer Group greenstones are deposited on top of the Luke Creek Group unconformably at about 2800 Ma (forming the Murchison Super Group).

Stage 5: Large volumes of monzogranite intrudes the base of the Murchison Super Group, forming contact metamorphic aureoles up to amphibolite grade at about 2690-2680 Ma.

Stage 6: Deformation phase 2; east-west trending, tight, upright folding.

Stage 7: Deformation phase 3; north-northwest to north-northeast trending, tight, isoclinal, upright folding. This was much more intense than the previous deformation phase.

Stage 8: Regional metamorphism of all the rocks up to greenschist facies at about 2680-2640 Ma.

Stage 9: Late intrusion of granitoid plutons into the greenstone belts and along the contacts of earlier intrusions at about 2640-2620 Ma.

Stage 10: Deformation phase 4; northwest to northeast trending, steeply dipping shear zones and faults. This is a continuation of deformation phase 3.

The Yalgoo Dome

In map view, the Yalgoo dome has an elliptoidal shape, elongate north-south, and is approximately 100 kilometres long and 50 kilometres wide.

Only a few studies have been done on the Yalgoo Dome itself, namely that of Myers and Watkins (1985), Rey *et al.* (1999), and various map sheets published by the Geological Survey of Western Australia. The thesis of which this review is part of, is in conjunction with a new project of the Geological Survey of Western Australia which is looking to re-map the Yalgoo area and discover the evolution of the Yalgoo Dome. Wider works from this effort include those by Van Kranendonk

et al. (2013) and Zibra (2012), which look at other areas in the Murchison Province. There have been various works done on the Yalgoo area, in particular looking at the Yalgoo Goldfields, which was discovered in 1894 (Muhling & Low 1977), but limited work has been done on the structural evolution of the dome.

Since the study by Macgregor (1951) where the granite-greenstone terrane in Zimbabwe was interpreted as diapiric batholiths being emplaced into a greenstone sequence, diapirism has become the popular theory to go to in order to explain granite-greenstone terranes (Myers & Watkins 1985). The Yilgarn Craton has been explained in using this theory in studies such as that by Gee (1979). Muhling and Low (1977) describe the Yalgoo Dome as low-grade metamorphic rocks in curved belts (greenstones), which are intruded by elliptical batholiths.

However, Myers and Watkins (1985) disagree with the diapiric emplacement theory for the Yalgoo Dome. Instead, they propose that the Yalgoo Dome and the elliptical granitoid intrusions found within it are dome-and-basin fold interference patterns. They describe the deformation history similar to that described by Watkins and Hickman (1990) , with D2 consisting of east-west trending folding and D3 consisting of sub-perpendicular, north-northwest to north-northeast trending

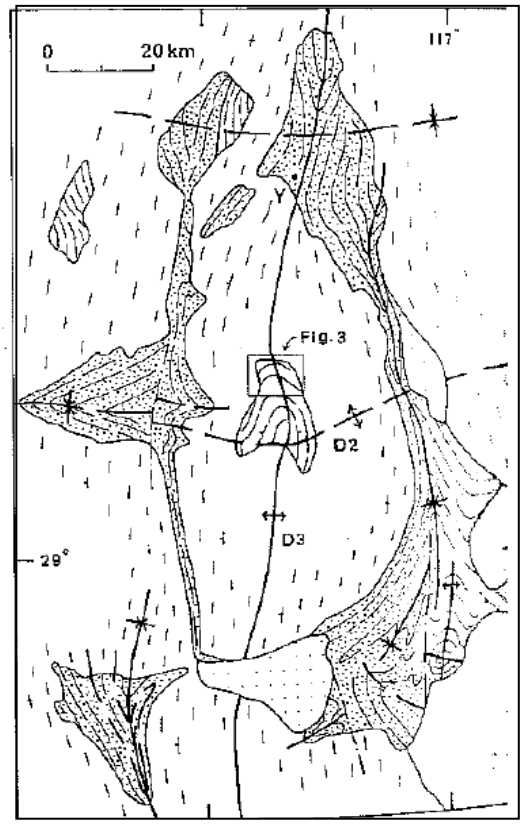

Figure 3 E-W trending D2 and E-W trending D3 as proposed by Myers and Watkins (1985).

folding (Figure 3). It is the interference patterns produced by these two deformation phases that produced the Yalgoo Dome.

Rey *et al.* (1999) found that for Myers and Watkins (1985) to be correct, a regional unconformity between D2 and D3, differing metamorphic grades and microstructures in the two axial planar fabrics, and consistent crosscutting relationships between D2 and D3 throughout the area must be seen in the field. None of these things are observed in the Murchison Province, and so Rey *et al.* (1999) concluded that Myers and Watkins (1985) were incorrect. Instead, Rey *et al.* (1999) proposes that the granite-greenstone patterns are formed through progressive incremental strain interference. They draw evidence from the field observations of consistent metamorphic grades and microstructures within a locality, the interference patterns only occurring locally where independent strain fields interact, and the cross-cutting relationships between two deformation phases are contradicting each other. From this, they suggest that it is the regional finite strain field that is seen in the Murchison Province that resulted in the granitic dome patterns, and was dominated by east-west shortening and north-south extension.

Conclusion:

The Yalgoo Dome is a little known structure in the Murchison Province of the Yilgarn Craton, with limited literature written about it. However, understanding the development of the dome could shed some further insights into the processes that form the patterns of granite-greenstone terranes, be it diapiric emplacement or fold interference. The study by Myers and Watkins (1985) suggested that the dome formed through fold interference patterns, however this was disagreed with by Rey *et al.* (1999), who suggested it formed through progressive incremental strain

interference. A few stratigraphic schemes have been proposed for the Murchison Domain, however Pidgeon and Hallberg (2000) concluded that no formal scheme could be constructed. There is much work still to do in the Yalgoo region, and the Geological Survey of Western Australia is currently undertaking further research area, in which the thesis that this review belongs to is in collaboration with.

References

ASPLER L. B. & CHIARENZELLI J. R. 1998. Two Neoarchean supercontinents? Evidence from the Paleoproterozoic. *Sedimentary Geology* **120**, 75-104.

AYRES L. D. 1983. Bimodal volcanism in Archean greenstone belts exemplified by greywacke composition, Lake Superior Park, Ontario. *Canadian Journal of Earth Sciences* **20**, 1168-1194.

BARLEY M. E., BEKKER A. & KRAPEZ B. 2005. Late Archean to Early Paleoproterozoic global tectonics, environmental change and the rise of atmospheric oxygen. *Earth and Planetary Science Letters* **238**, 156-171.

BURKE K., DEWEY J. F. & KIDD W. S. F. 1976. Dominance of horizontal movements, arc and microcontinental collisions during the later permobile regime. Paper presented at The early history of the Earth(unpubl.).

CANN J. R. 1974. A model for oceanic crustal structure developed. *Geophysical Journal of the Royal Astronomical Society* **39**, 169-187.

CHAVAGNAC V. 2004. A geochemical and Nd isotopic study of Barberton komatiites (South Africa): Implication for the Archean mantle. *Lithos* **75**, 253-281.

CHOUKROUNE P., BOUHALLIER H. & ARNDT N. T. 1995. Soft lithosphere during periods of Archaean crustal growth or crustal reworking. *Geological Society Special Publications* **95**, 67-86.

COLLINS W. J. & VAN KRANENDONK M. J. 1998. Partial convective overturn of Archaean crust in the East Pilbara Craton, Western Australia; driving mechanisms and tectonic implications. *Journal of Structural Geology* **20**, 1405-1424.

COLTICE N., BERTRAND H., REY P., JOURDAN F., PHILLIPS B. R. & RICARD Y. 2009. Global warming of the mantle beneath continents back to the Archaean. *Gondwana Research* **15**, 254-266.

DAVIES G. F. 1995. Punctuated tectonic evolution of the Earth. *Earth and Planetary Science Letters* **136**, 363-379.

DAVIES G. F. 1998. Plates, plumes, mantle convection, and mantle evolution. Paper presented at The Earth's mantle; composition, structure, and evolution(unpubl.).

DAVIES G. F. 2006. Gravitational depletion of the early Earth's upper mantle and the viability of early plate tectonics. *Earth and Planetary Science Letters* **243**, 376-382.

DE RONDE C. E. J. & DE WIT M. J. 1994. Tectonic history of the Barberton greenstone belt, South Africa: 490 million years of Archean crustal evolution. *Tectonics* **13**, 983-1005.

DEWEY J. F. & WINDLEY B. F. 1981. Growth and differentiation of the continental crust. *Philosophical Transactions of the Royal Society of London, Series A: Mathematical and Physical Sciences* **301**, 189-206.

DIMROTH E., IMREH L., COUSINEAU P., LEDUC M. & SANSCHAGRIN Y. 1985. Paleogeographic analysis of mafic submarine flows and its use in the exploration for massive sulphide deposits. *Special Paper - Geological Association of Canada* **28**, 203-222.

DIMROTH E., IMREH L., ROCHELEAU M. & GOULET N. 1982. Evolution of the south-central part of the Archean Abitibi Belt, Quebec; Part I, Stratigraphy and paleogeographic model. *Canadian Journal of Earth Sciences = Journal Canadien des Sciences de la Terre* **19**, 1729-1758.

FISHER R. V. 1982. Debris flows and lahars. *Short Course Notes - Geological Association of Canada* **2**, 136-220.

FOLEY B. J. 1997. Reassessment of the Archean tectonics in the Murchison Province, Western Australia. *Abstracts - Geological Society of Australia* **46**, 23.

FRASER G., MCAVANEY S., NEUMANN N., SZPUNAR M. & REID A. 2010. Discovery of early Mesoarchean crust in the eastern Gawler Craton, South Australia. *Precambrian Research* **179**, 1-21.

GEE R. D. 1979. Structure and tectonic style of the Western Australian Shield. *Tectonophysics* **58**, 327-369.

GEE R. D., BAXTER J. L., WILDE S. A. & WILLIAMS I. R. 1981. Crustal development in the Archaean Yilgarn Block, Western Australia. *Special Publication - Geological Society of Australia*, 43-56.

GOODWIN A. M. 1976. Archean volcanoes in southwestern Abitibi Belt, Canada; form, composition and development. *Abstracts with Programs - Geological Society of America* **8**, 888.

HAMILTON W. B. 1998. Archean magmatism and deformation were not products of plate tectonics. *Precambrian Research* **91**, 143-179.

HAMILTON W. B. 2011. Plate tectonics began in Neoproterozoic time, and plumes from deep mantle have never operated. *Lithos* **123**, 1-20.

HERZBERG C. 1992. Depth and degree of melting of komatiites. *Journal of Geophysical Research: Solid Earth* **97**, 4521-4540.

HICKMAN A. H. 2004. Two contrasting granite-greenstone terranes in the Pilbara Craton, Australia; evidence for vertical and horizontal tectonic regimes prior to 2900 Ma. *Precambrian Research* **131**, 153-172.

HOFFMAN P. F. & RANALLI G. 1988. Archean oceanic flake tectonics. *Geophysical Research Letters* **15**, 1077-1080.

JOHNSON S. E., DUPEE M. E. & GUIDOTTI C. V. 2006. Porphyroblast rotation during crenulation cleavage development; an example from the aureole of the Mooselookmeguntic Pluton, Maine, USA. *Journal of Metamorphic Geology* **24**, 55-73.

KRONER A. & LAYER P. W. 1992. Crust formation and plate motion in the early Archean. *Science* **256**, 1405-1411.

MACGREGOR A. M. 1951. Some milestones in the Precambrian of Southern Rhodesia [presidential address]. *Proceedings of the Geological Society of South Africa*.

MUHLING P. C. & LOW G. H. 1977. Yalgoo, Western Australia. *1:250 000 Explanatory Notes*.

MYERS J. S. & PLATT R. G. 1977. Mineral chemistry of layered Archaean anorthosite at Majorqap qava, near Fiskenaesset, Southwest Greenland. *Lithos* **10**, 59-72.

MYERS J. S. & WATKINS K. P. 1985. Origin of granite- greenstone patterns, Yilgarn Block, Western Australia. *Geology* **13**, 778-780.

NESBITT R. W., SUN S. S. & PURVIS A. C. 1979. Komatiites; geochemistry and genesis. *The Canadian Mineralogist* **17, Part 2**, 165-186.

NISBET E. G. & FOWLER C. M. R. 1983. Model for Archean plate tectonics. *Geology* **11**, 376-379.

PARMAN S. W., DANN J. C., GROVE T. L. & DE WIT M. J. 1997. Emplacement conditions of komatiite magmas from the 3.49 Ga Komati Formation, Barberton Greenstone Belt, South Africa. *Earth and Planetary Science Letters* **150**, 303-323.

PATERSON S. R., VERNON R. H. & TOBISCH O. T. 1989. A review of criteria for the identification of magmatic and tectonic foliations in granitoids. *Journal of Structural Geology* **11**, 349-363.

PIDGEON R. T. & HALLBERG J. A. 2000. Age relationships in supracrustal sequences of the northern part of the Murchison Terrane, Archaean Yilgarn Craton, Western Australia; a combined field and zircon U-Pb study. *Australian Journal of Earth Sciences* **47**, 153-165.

REY P., COSTA S., VANDERHAEGHE O. & FOLEY B. 1999. Archaean regional strain field in the Yilgarn Craton (WA); fold superposition or incremental strain field interferences? *Abstracts - Geological Society of Australia* **53**, 221-222.

SHIREY S. B. & RICHARDSON S. H. 2011. Start of the Wilson Cycle at 3 Ga Shown by Diamonds from Subcontinental Mantle. *Science* **333**, 434-436.

SIZOVA E., GERYA T. & BROWN M. in press. Contrasting styles of Phanerozoic and Precambrian continental collision. *Gondwana Research*.

SLEEP N. H. & WINDLEY B. F. 1982. Archean plate tectonics: constraints and inferences. *Journal of Geology* **90**, 363-379.

TAIRA A., PICKERING K. T., WINDLEY B. F. & SOH W. 1992. Accretion of Japanese island arcs and implications for the origin of Archean greenstone belts. *Tectonics* **11**, 1224-1244.

TARNEY J. & WINDLEY B. F. 1981. Marginal basins through geological time. *Philosophical Transactions of the Royal Society of London, Series A: Mathematical and Physical Sciences* **301**, 217-232.

THOMPSON STIEGLER M., COOPER M., BYERLY G. R. & LOWE D. R. 2012. Geochemistry and petrology of komatiites of the Pioneer Ultramafic Complex of the 3.3 Ga Weltevreden Formation, Barberton greenstone belt, South Africa. *Precambrian Research* **212–213**, 1-12.

VAN KRANENDONK M. J. 2010. Two types of Archean continental crust: plume and plate tectonics on early earth. *American Journal of Science* **310**, 1187-1209.

VAN KRANENDONK M. J. 2011. Onset of Plate Tectonics. *Science* **333**, 413-414.

VAN KRANENDONK M. J., COLLINS W. J., HICKMAN A. & PAWLEY M. J. 2004. Critical tests of vertical vs. horizontal tectonic models for the Archaean East Pilbara Granite–Greenstone Terrane, Pilbara Craton, Western Australia. *Precambrian Research* **131**, 173-211.

VAN KRANENDONK M. J., HUGH SMITHIES R., HICKMAN A. H. & CHAMPION D. C. 2007. Review: secular tectonic evolution of Archean continental crust: interplay between horizontal and vertical processes in the formation of the Pilbara Craton, Australia. *Terra Nova* **19**, 1-38.

VAN KRANENDONK M. J., IVANIC T. J., WINGATE M. T. D., KIRKLAND C. L. & WYCHE S. 2013. Long-lived, autochthonous development of the archean murchison domain, and implications for yilgarn craton tectonics. *Precambrian Research* **229**, 49-92.

WATKINS K. P. & HICKMAN A. H. 1990. Excursion no. 2: Murchison granite-greenstone terrain. Part 1: Geology of the Murchison Province granite-greenstone terraine, Western Australia. Paper presented at Third international Archaean symposium, Perth, 1990, excursion guidebook(unpubl.).

WEINBERG R. 2005. Kinematic history of the Boulder-Lefroy shear zone system and controls on associated gold mineralization, Yilgarn craton, Western Australia. *Economic Geology and the Bulletin of the Society of Economic Geologists* **100**, 1407-1426.

WEINBERG R. F. & MARK G. 2008. Magma migration, folding, and disaggregation of migmatites in the Karakoram shear zone, Ladakh, NW India. *Geological Society of America Bulletin* **120**, 994-1009.

WEINBERG R. F., MORESI L. & VAN DER BORGH P. 2003. Timing of deformation in the Norseman-Wiluna Belt, Yilgarn Craton, Western Australia. *Precambrian Research* **120**, 219-239.

WEINBERG R. F. & VAN DER BORGH P. 2008. Extension and gold mineralization in the Archean Kalgoorlie Terrane, Yilgarn Craton. *Precambrian Research* **161**, 77-88.

WEINBERG R. F., VAN DER BORGH P., BATEMAN R. J. & GROVES D. I. 2005. Kinematic history of the Boulder-Lefroy shear zone system and controls on associated gold mineralization, Yilgarn Craton, Western Australia. *Economic Geology and the Bulletin of the Society of Economic Geologists* **100**, 1407-1426.

WELLS P. R. A. 1979. Chemical and thermal evolution of Archaean sialic crust, southern West Greenland. *Journal of Petrology* **20**, 187-226.

WINDLEY B. F. 1993. Uniformitarianism today: plate tectonics is the key to the past. *Journal - Geological Society (London)* **150**, 7-19.

WINDLEY B. F. & DAVIES F. B. 1978. Volcano spacings and lithospheric/crustal thickness in the Archaean. *Earth and Planetary Science Letters* **38**, 291-297.

YIN A. 2004. Gneiss domes and gneiss dome systems. *Special Paper - Geological Society of America* **380**, 1-14.

ZEGERS T. E., NELSON D. R., WIJBRANS J. R. & WHITE S. H. 2001. SHRIMP U-Pb zircon dating of Archean core complex formation and pancratonic strike-slip deformation in the East Pilbara Granite-Greenstone Terrain. *Tectonics* **20**, 883-908.

ZEGERS T. E., WIJBRANS J. R. & WHITE S. H. 1999. 40Ar/39Ar age constraints on tectonothermal events in the Shaw area of the eastern Pilbara granite–greenstone terrain (W Australia): 700 Ma of Archean tectonic evolution. *Tectonophysics* **311**, 45-81.

ZIBRA I. 2012. Syndeformational granite crystallisation along the Mount Magnet greenstone belt, Yilgarn Craton; evidence of large-scale magma-driven strain localisation during Neoarchean time. *Australian Journal of Earth Sciences* **59**, 793-806.

APPENDIX C - SHRIMP Dating Results

209689 (ZIBRA; metatonalite, BADJA): 23 analyses of 18 zircons

- Zircons from this sample are colourless to dark brown and mainly subhedral. In CL images, concentric zoning is ubiquitous, and many crystals contain high-U, metamict zones
- Seven analyses >25% discordant (Group D) are not considered further
- Fifteen analyses (Group I) yield a discordia regression, with intercepts at 2960 ± 10 and 510 ± 220 Ma (MSWD = 1.04)
- One analysis (Group P) yields a $^{207}Pb^*/^{206}Pb^*$ date of 2857 ± 30 Ma (1σ), interpreted to reflect ancient loss of radiogenic Pb (a second analysis of this zircon yields a highly discordant result)
- The date of **2960 ± 10 Ma** is interpreted as the magmatic crystallization age of the tonalite protolith

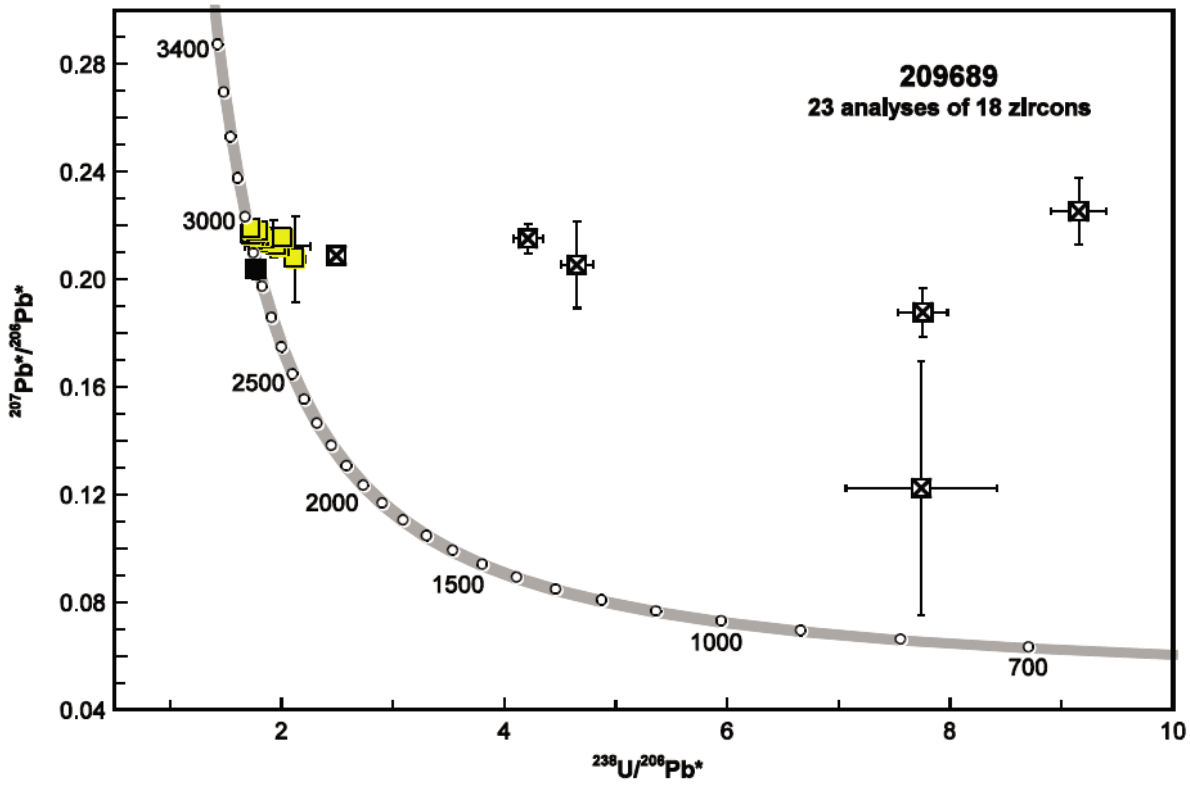

Figure 1. U–Pb analytical data for zircons from sample 209689: metatonalite, BADJA. Yellow squares indicate Group I (magmatic zircons); black square indicates Group P (radiogenic-Pb loss); crossed squares indicate Group D (discordance >25%). One highly imprecise analysis in Group D is not shown.

Geochronologists: Wingate, Kirkland

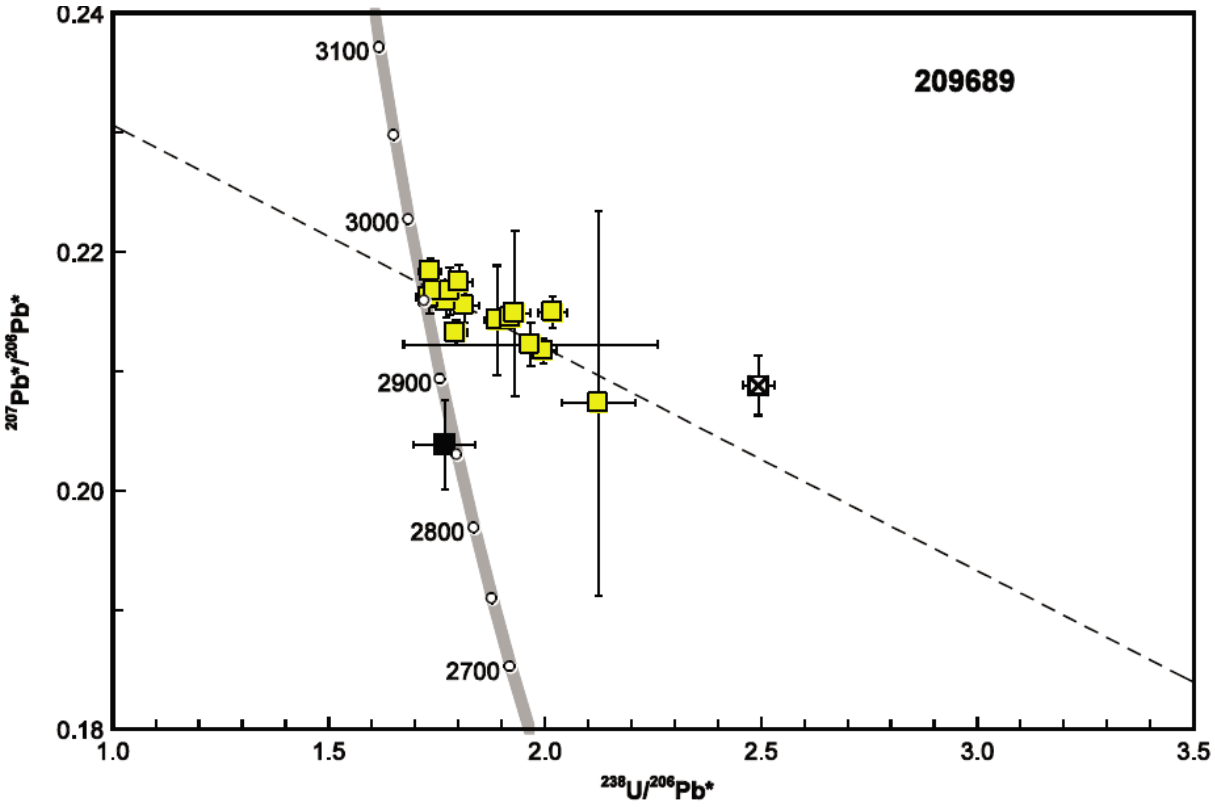

Figure 2. Expanded view of U–Pb analytical data for zircons from sample 209689: metatonalite, BADJA. The dashed line indicates a regression through data in Group I. Symbols as in Fig. 1.

Geochronologists: Wingate, Kirkland


[G13-33] 209689_1
100 µm
500 µm
50 40 30 25
uranotherite ?
U, Th, no Zr
Ø = high 204Pb
[G13-33] 209689_1

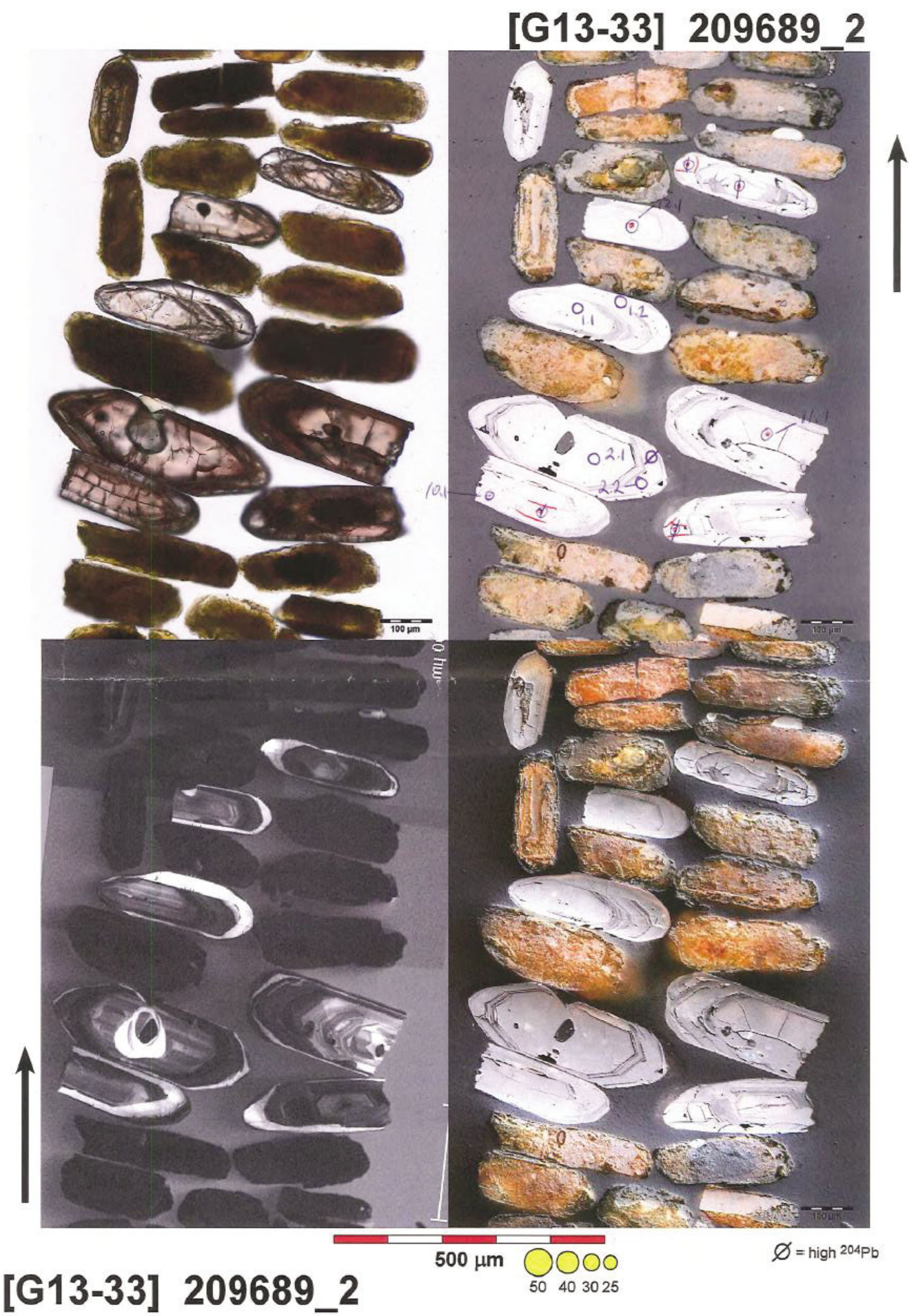
[G13-33] 209689_2
100 µm
500 µm
50 40 30 25
Ø = high 204Pb
[G13-33] 209689_2

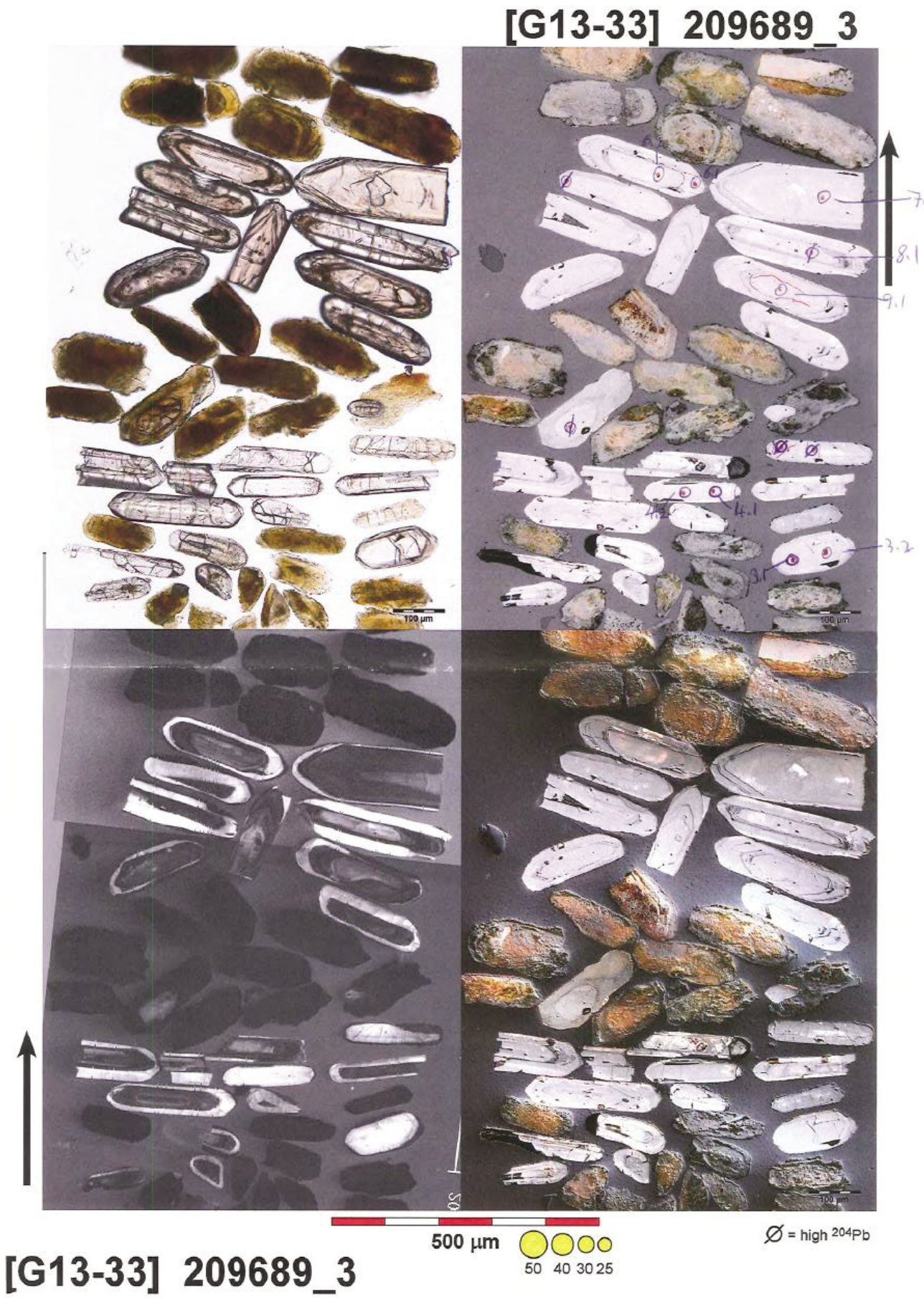
[G13-33] 209689_3
7.1
8.1
9.1
4.1
3.2
3.1
100 µm
500 µm
50 40 30 25
Ø = high 204Pb
[G13-33] 209689_3

155858 (ZIBRA; granite, BADJA): 5 analyses of 5 zircons

- Zircons from this sample are colourless to dark brown and mainly subhedral. In CL images, concentric zoning is ubiquitous, and most crystals are dominated by high-U, metamict zones
- Only five zircons could be analysed successfully, owing to very high common Pb contents
- Five analyses (Group I) yield a weighted mean $^{207}Pb^*/^{206}Pb^*$ date of **2752 ± 13 Ma** (MSWD = 1.3), interpreted as the magmatic crystallization age of the granite

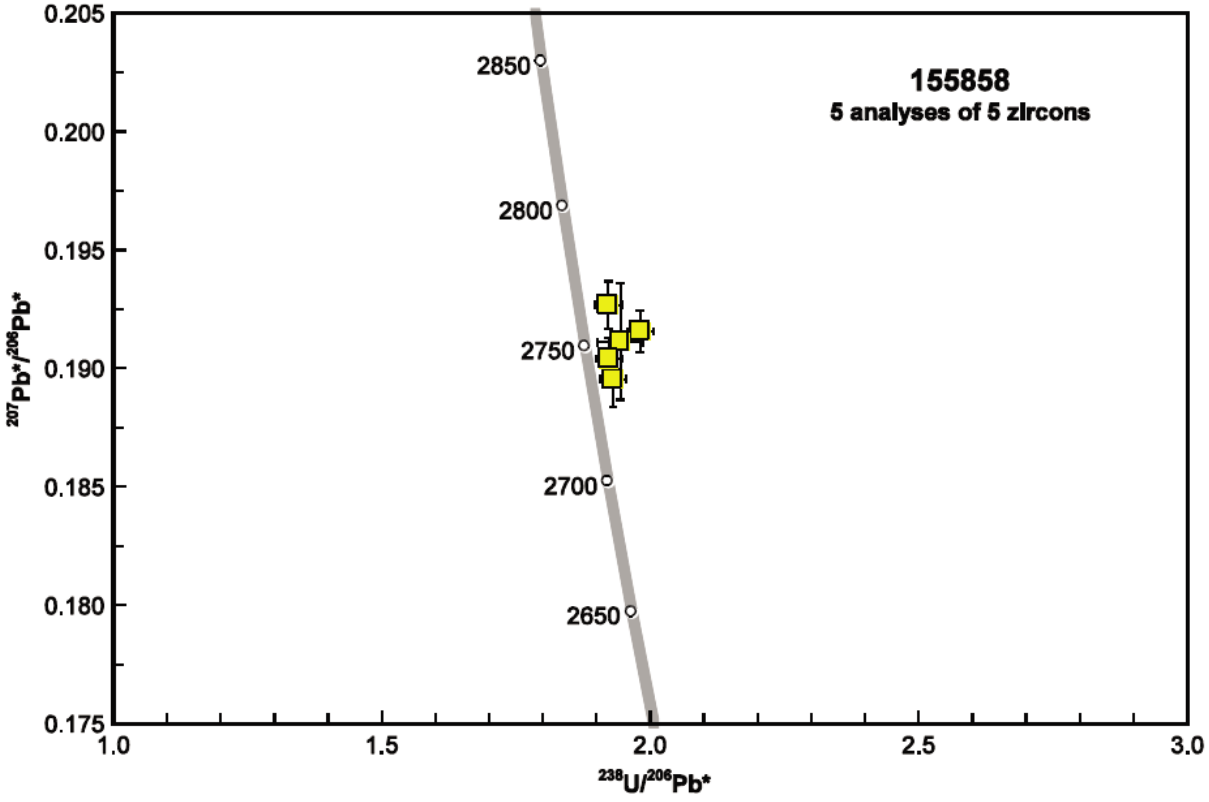

Figure 1. U–Pb analytical data for zircons from sample 155858: granite, BADJA. Yellow squares indicate Group I (magmatic zircons).

Geochronologists: Wingate, Kirkland


[G13-33] 155858_1
3.1
2.1
1.1
100 µm
500 µm
50 40 30 25
Ø = high 204Pb
[G13-33] 155858_1

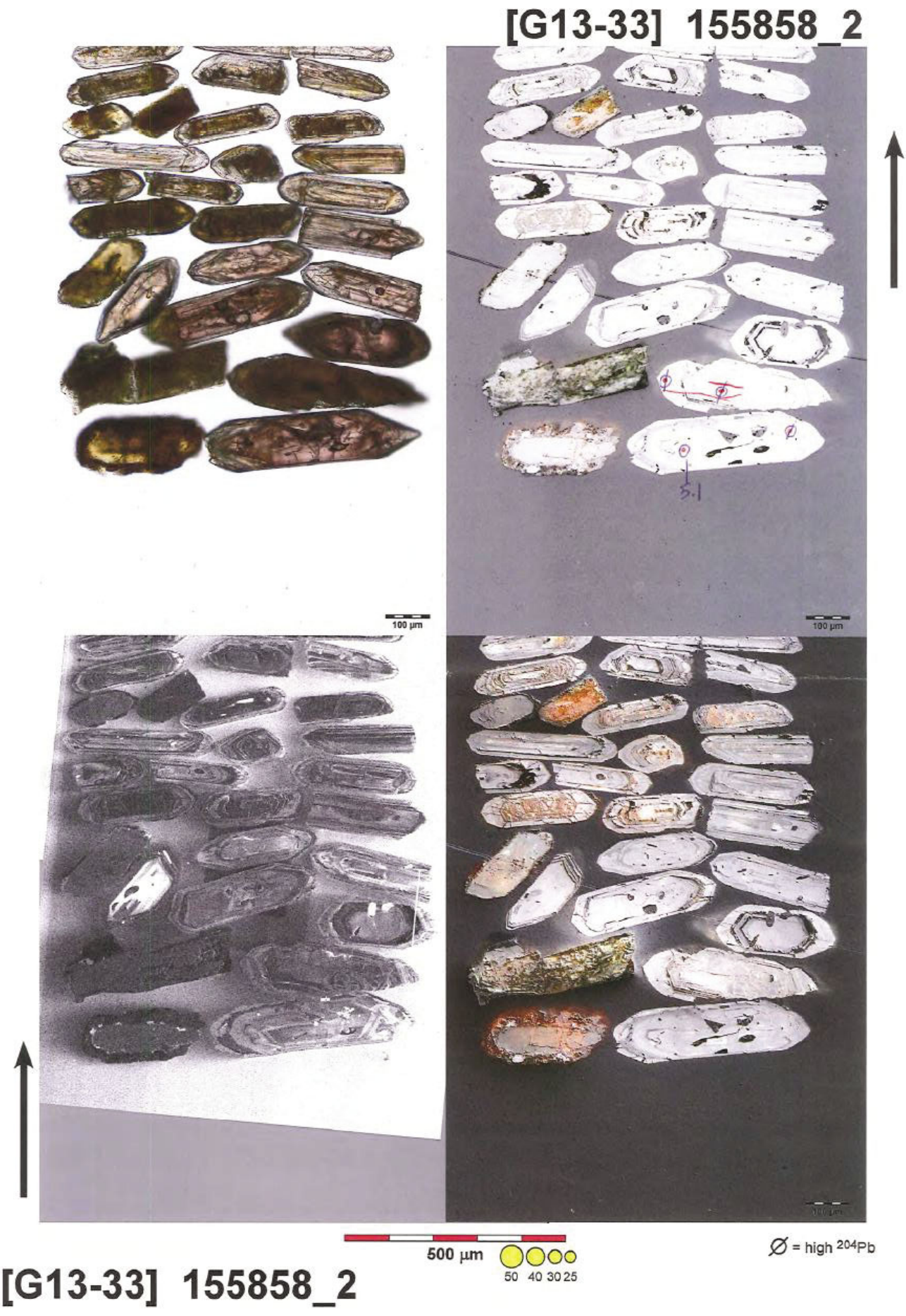
[G13-33] 155858_2
100 µm
100 µm
500 µm
50 40 30 25
∅ = high 204Pb
[G13-33] 155858_2

$^{232}Th/^{238}U$	f_{204} (%)	$^{238}U/^{206}Pb$ ±1 σ		$^{207}Pb/^{206}Pb$ ±1 σ		$^{238}U/^{206}Pb^*$ ±1 σ		$^{207}Pb^*/^{206}Pb^*$ ±1 σ		$^{238}U/^{206}Pb^*$ date (Ma) ±1 σ		$^{207}Pb^*/^{206}Pb^*$ date (Ma) ±1 σ		Disc (%)
0.49	0.934	1.913	0.024	0.19788	0.00080	1.931	0.024	0.18955	0.00119	2690	28	2738	10	1.8
0.60	0.245	1.918	0.024	0.19257	0.00078	1.923	0.024	0.19039	0.00087	2700	27	2746	8	1.7
0.51	0.871	1.928	0.041	0.19889	0.00179	1.945	0.042	0.19112	0.00246	2674	48	2752	21	2.8
0.27	0.345	1.976	0.024	0.19463	0.00074	1.982	0.024	0.19156	0.00090	2633	26	2756	8	4.5
0.97	0.345	1.915	0.025	0.19575	0.00083	1.922	0.025	0.19267	0.00101	2701	29	2765	9	2.3
0.12	0.449	2.115	0.086	0.21135	0.01584	2.124	0.086	0.20735	0.01608	2487	87	2885	126	13.8
0.37	0.363	1.990	0.029	0.21494	0.00093	1.997	0.029	0.21171	0.00108	2617	31	2919	8	10.3
0.48	-0.042	1.968	0.294	0.21189	0.00174	1.967	0.294	0.21226	0.00176	2650	371	2923	13	9.3
0.61	0.096	1.793	0.026	0.21410	0.00100	1.795	0.026	0.21324	0.00104	2855	33	2930	8	2.6
0.51	0.698	1.877	0.030	0.22048	0.00448	1.890	0.030	0.21428	0.00461	2737	36	2938	35	6.8
0.02	0.534	1.912	0.022	0.21925	0.00072	1.922	0.022	0.21451	0.00090	2700	26	2940	7	8.2
0.60	0.469	1.922	0.035	0.21903	0.00683	1.931	0.035	0.21487	0.00693	2690	41	2943	52	8.6
0.52	0.294	2.012	0.033	0.21756	0.00121	2.018	0.033	0.21495	0.00135	2595	35	2943	10	11.8
0.61	0.065	1.813	0.033	0.21609	0.00142	1.814	0.033	0.21551	0.00146	2831	42	2947	11	4.0
0.48	0.196	1.769	0.030	0.21757	0.00120	1.772	0.030	0.21583	0.00129	2884	40	2950	10	2.2
0.58	0.094	1.732	0.030	0.21704	0.00126	1.734	0.030	0.21620	0.00130	2936	42	2953	10	0.6
0.68	0.061	1.745	0.031	0.21722	0.00124	1.746	0.031	0.21668	0.00127	2919	42	2956	9	1.3
0.50	0.326	1.775	0.037	0.21960	0.00177	1.781	0.037	0.21671	0.00200	2873	50	2956	15	2.8
0.77	0.341	1.796	0.032	0.22050	0.00128	1.802	0.032	0.21747	0.00144	2845	41	2962	11	3.9
0.80	0.147	1.733	0.025	0.21968	0.00100	1.735	0.025	0.21838	0.00106	2934	34	2969	8	1.2
0.43	21.056	6.114	0.432	0.30716	0.01037	7.745	0.678	0.12242	0.04721	783	70	1992	686	60.7
0.57	0.489	5.551	9.572	0.17680	0.13405	5.578	9.619	0.17223	0.13509	1083	-2896	2579	1310	58.8
0.12	4.044	7.442	0.202	0.22380	0.00421	7.756	0.222	0.18774	0.00914	782	22	2722	80	71.3
0.30	20.110	3.717	0.096	0.38391	0.00415	4.652	0.144	0.20533	0.01604	1255	36	2869	127	56.3
0.52	2.805	2.424	0.036	0.23377	0.00130	2.494	0.037	0.20883	0.00250	2173	28	2896	19	25.0
0.49	1.013	4.171	0.129	0.22410	0.00410	4.214	0.131	0.21511	0.00556	1373	40	2944	42	53.4
0.21	6.649	8.549	0.206	0.28407	0.00453	9.158	0.250	0.22520	0.01240	668	18	3018	88	77.9
0.05	0.144	1.766	0.071	0.20515	0.00351	1.768	0.072	0.20386	0.00374	2890	97	2857	30	-1.1

RECORD 2014/4

STRUCTURAL EVOLUTION OF THE YALGOO DOME, YILGARN CRATON, WESTERN AUSTRALIA

Caudery

This Record is published in digital format (PDF) and is available as a free download from the DMP website at <www.dmp.wa.gov.au/GSWApublications>.

Further details of geological products produced by the Geological Survey of Western Australia can be obtained by contacting:

Information Centre
Department of Mines and Petroleum
100 Plain Street
EAST PERTH WESTERN AUSTRALIA 6004
Phone: (08) 9222 3459 Fax: (08) 9222 3444
www.dmp.wa.gov.au/GSWApublications